Vietnamese-German University

COPYRIGHT WARNING

This paper is protected by copyright. You are advised to print or download **ONE COPY** of this paper for your own private reference, study and research purposes. You are prohibited having acts infringing upon copyright as stipulated in Laws and Regulations of Intellectual Property, including, but not limited to, appropriating, impersonating, publishing, distributing, modifying, altering, mutilating, distorting, reproducing, duplicating, displaying, communicating, disseminating, making derivative work, commercializing and converting to other forms the paper and/or any part of the paper. The acts could be done in actual life and/or via communication networks and by digital means without permission of copyright holders.

The users shall acknowledge and strictly respect to the copyright. The recitation must be reasonable and properly. If the users do not agree to all of these terms, do not use this paper. The users shall be responsible for legal issues if they make any copyright infringements. Failure to comply with this warning may expose you to:

- Disciplinary action by the Vietnamese-German University.
- Legal action for copyright infringement.
- Heavy legal penalties and consequences shall be applied by the competent authorities.

The Vietnamese-German University and the authors reserve all their intellectual property rights.

RUHR-UNIVERSITÄT BOCHUM

Vietnamese-German University

TOPIC

OPTIMIZATION OF ELECTRODE DESIGNS AND OPERATING PARAMETERS FOR EFFECTIVE CAPACITIVE DEIONIZATION

BINH DUONG 2021

Submitted by: Pham Nhat Nhien

RUB Student ID: 108018207573

VGU Student ID: 11071

Supervisor: Prof. Dr. Tran Le Luu

Co-supervisor: N.A.

Ruhr – Universität Bochum
Vietnamese – German University

Optimization of electrode designs and operating parameters for effective capacitive deionization

Thesis for degree of

BACHAELOR OF ENGINEERING

By

Pham Nhat Nhien – ID: 11071

Supervisor: Dr. Tran Le Luu

Binh Duong, September 2021

Affirmation

I hereby declare that this report (including diagrams, drawings, sketches etc.) is a product of my own work, unless otherwise referenced. All opinions, results, conclusions and recommendations are of my own and may not represent the policies and opinions of the Vietnamese-German University.

Pham Nhat Nhien

Acknowledgement

This thesis paper would not have been accomplished without the guidance of my supervisor Prof. Tran Le Luu, who had been extremely understanding with his advice and support. I would also like to extend my gratitude to all the VGU chemistry laboratory staffs that allow me to conduct my experimentation as well as their willingness to share insight on this topic. My final sincere thanks go to my faculty coordinator and assistant Prof. Tran Trung Thanh and Ms. Nguyen Thi Tuu who have provide much aid throughout my years at VGU.

Abstracts

With the growing demand for fresh water, especially in regions that are currently suffering from seawater intrusion in Vietnam, development of an effective, cost-saving and environmentally friendly desalination system is crucial. Capacitive deionization (CDI) is a relatively new technology, and yet has shown a lot of potential to be the ideal solution of our water problem. In this study, we first review the science behind the CDI technology including its operation principles and strategies for performance advancement.

Further investigation is then established by constructing three lab-scale CDI models with multiple electrode pairs undergoing various operating conditions. Results documented in this paper provide insight to how different design metrics affect the system performance and act as a framework for future reference. Favorable performance of the triple electrode pairs CDI is achieved with adsorption capacity of 11.3 mg/g. Additionally, by implementing both zero voltage discharge (ZVD) and reverse voltage discharge (RVD) method during desorption cycle, higher electrode regeneration rate is observed and energy consumption during discharge period is cut by half.

Keywords: Capacitive deionization (CDI), Water desalination, Active carbon electrode, Performance optimization.

Table of Contents

Affirmation i
Acknowledgement ii
Abstracts iii
Table of Contents iv
List of Figures vi
List of Tables viii
1. Introduction 1
1.1. Problem description 1
1.1.1. Water status in Vietnam 1
1.1.2. Salt water intrusion problem in Vietnam 2
1.2. Desalination technologies in Vietnam 3
1.2.1. Thermal process 4
1.2.2. Membrane process 5
1.2.3. Electrodyalysis (ED) 6
1.2.4. Capacitive deionization (CDI) 7
2. Literature review 8
2.1. Experimental and development approaches in recent CDI studies 8
2.2. Theoretical and technical background 10
2.2.1. Basic designs and operations 10
2.2.2. Electrodialysis behaviors in CDI 11
2.2.3. Faradaic reactions 14
2.3. Electrode technology 16
2.3.1. The science of electrode porosity on desalination performance 22
2.3.2. Surface modification methods for improving electrode properties 23
2.4. Comparision of different types of CDI 16
2.4.1. Flow-by and flow-through CDI. 16
2.4.2. Asymmetric and symmetric CDI 18
2.5. Effects of various infeed concentration on desalination performance 33

2.5.1. Constant voltage and constant current operation mode 20
2.6. CDI in industrial scale application 26
2.6.1. Stacking effect of scale up CDI system 26
2.6.2. Single-pass mode and batch mode for CDI analysis 27
3. Methodology 29
3.1. CDI cell preparation 29
3.2. Feedwater preparation 30
3.3. Equipment setup 30
3.4. Experiment description 31
3.5. Performance parameter 31
3.5.1. Water quality 31
3.5.2. Energy efficiency 32
3.5.3. Electrode regeneration rate 32
4. Results 33
4.1. Effects of applied voltage difference on desalination performance 33
4.2. Effects of changing flow rate on desalination performance 41
4.3. Effects of different discharging mode on desalination performance 45
5. Conclusion 48
6. Referrences **Error! Bookmark not defined.**

List of Figures

Figure 1. Water usage in different industries in Vietnam (2012) [1] 2

Figure 2. Distribution of desalination technologies worldwide [8] 3

Figure 3. Schematic design of the multi-stage flash distillation (MSF) system [10] 4

Figure 4. Description of a) normal osmosis flow and b) reverse osmosis flow [11] 5

Figure 5. Example of an electrodialysis plant [13] 6

Figure 6. Description of CDI operating principle during (a) charging (absorption) phase and (b) discharging (desorption) phase Figure 7. Demonstration of how ion exchange membrane operates [41] 10

Figure 7. Demonstration of how ion exchange membrane operates [41] 11

Figure 8. Description of electrical double layers (EDL) formation on one electrode in an infinite fluid body [43] 12

Figure 9. Ions distribution between CDI's electrodes [43] 13

Figure 10. Schematic description of CDI system with (a) non-overlapping EDL and (b) overlapping EDL [43] 14

Figure 11. Comparison of different flow mode: (a) flow-by CDI and (b) flow-through CDI [26] 17

Figure 12. Potential distribution of symmetrical and asymmetrical CDI [27] 19

Figure 13. Comparison of: voltage (a) and current (b) of CV mode; voltage and current (d) of CC mode; voltage (e) and current (f) of SV mode [25, 80] 21

Figure 14. Description of electrical equivalent of (a) parallel stacking CDI and (b) series stacking CDI [81] 26

Figure 15. Description of (a) single-pass mode operation and (b) effluent conductivity value vs. time in single-pass mode [41] 27

Figure 16. Description of (a) batch mode operation and (b) effluent conductivity value vs. time in batch mode [41] 28

Figure 17. Assembly representation of a CDI unit cell with (a) one pair of electrodes, (b) two pairs of electrodes and three pairs of electrodes 29

Figure 18. Description of CDI analysis experiment set up 30

Figure 19. Effluent concentration at exit for different TDS feed water (Flow rate: 400mL/min; applied voltage: 1.2V; WR 66.7%) 34

Figure 20. Electric behavior of different initial concentration operation 35

Figure 21. Comparison of different infeed TDS regarding: a) total mass adsorbed, b) removal rate and c) energy consumption. 36

Figure 22. Effluent concentration at exit for different adsorption and desorption voltage (flow rate: 400mL/min; initial TDS: 600ppm; 66.7% WR) 37

Figure 23. Electrical behavior of different applied voltage operation. 38

Figure 24. Comparison of different applied voltages regarding: a) total mass adsorbed, b) removal ratio and c) energy consumption. 39

Figure 25. Effluent concentration at exit for different flow rate (Initial TDS: 600ppm; applied voltage: 1.2V; WR 66.7%) 40

Figure 26. Electrical behavior of different flow rate operation. 41

Figure 27. Comparison of different flow rate regarding: a) energy consumption per ion mass and b) energy consumption per volume 42

Figure 28. Comparison of different flow rate regarding: a) salt adsorbed and b) removal rate 42

Figure 29. Effluent concentration at exit during desorption phase for discharge mode 44

Figure 30. Comparison of different discharge mode regarding: a) electrode regeneration rate and b) energy consumption 44

List of Tables

Table 1. Data of surface water supplies in Vietnam, 2012 [1] 1

Table 2. Water classification based on salt concentration [5] 3

Table 3. Comparison of different desalination methods 7

Table 4. Common base materials for CDI electrode 9

Table 5. List of possible Faradaic reactions 15

Table 6. Potential of zero charge (E_{pzc}) value of some electrode material 18

Table 7. Characteristic of commonly found salt ions 23

Table 8. Comparison of different metal oxide coating surface modification 24,25

Table 9. Comparison of different chemical treatment surface modification 25

Table 10. Specification of experiment CDI cell 29

Table 11. Comparison of initial concentration effect with other studies 36

Table 12. Comparison of applied voltage effects with other studies 39

Table 13. Comparison of flow rate effects with other studies 43

Table 14. Comparison of discharging mode effects with other study 45

1. Introduction

1.1. Problem description

1.1.1. Water status in Vietnam

Water for millennials has been the most imperative resource in history that contributes in every aspect of human life from hydration needs to agricultural and production impact. Yet, access for fresh water is not always available with only 3% of the Earth's water being freshwater and approximately 30% of that freshwater is attainable through rivers, lakes and underground water sources [1] . The remaining freshwater available is locked in glacier and polar ice caps, therefore cannot be accessed for consumption. Being a country with dense river and lake network, Vietnam majors its source of freshwater from the abundance of water bodies located in the Red River valley and the Mekong Delta regions. The amount of water supply is heavily dependent on the annual flow which provide renewable water resources each year. Table 1 includes information of the surface water (from rivers, lakes, etc.) that are available in Vietnam, note that only the lower stream can be sourced locally since majority of the upper stream are in foreign countries.

Table 1. Data of surface water supplies in Vietnam, 2012 [1].

	Water body area (km^2)	**Annal flow 2012 ($billion\ m^3/year$)**
Upper stream	871,490	526
Lower stream	225,620	315
Total	1,097,110	841

In 2012, the Vietnam Environment Administration reported the fresh water supply per capita of 4,000m3 per year , however this number is expected to decrease to 3,100 m3 by 2025 [2]. Meanwhile, the worldwide average water supply is 7,400m3 and the IWRA water supply standard of 10,000m3/person/year for countries with moderate water resources. Combined with a dense population of 90 million, heavily-dependent-on-agricultural economy, the country is now facing the risk of water crisis with the annual water flow from major river and lake systems exhibit constant decrease from 2006 to 2011 [2]. In addition, water quality is also a chronic problem Vietnam is facing. The country's water contamination of the already diminishing water resources is caused by either excessive waste from

production or environment effects like sea intrusion and climate change present further threat of hazardous consumption to personal health.

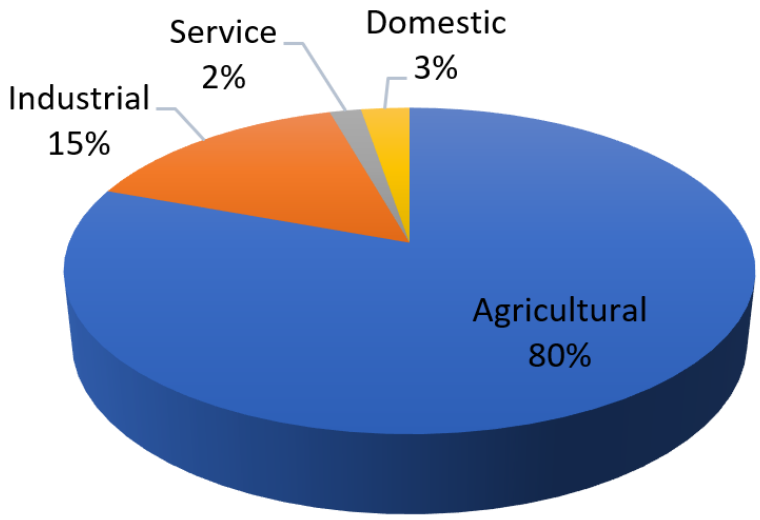

Figure 1. Water usage in different industries in Vietnam (2012) [1].

1.1.2. Salt water intrusion problem in Vietnam

Sea intrusion is a phenomenon that occurs in coastal areas when sea level rises and enters the fresh water reservoirs that leads to high salt concentration contamination of water and soil. This happen naturally and annually because the lack of fresh water induces rising sea level through osmosis mechanism. Saline water with higher content of salt and mineral ions will exert higher hydraulic pressure due to its higher density. Therefore, when there is lower volume of freshwater during the dry seasons, seawater will invade toward inland in order to balance the pressure difference.

The effects of global warming and climate change also contributes to the melting of iceberg in both the North and South Poles and increasing the total mass volume of seawater. In 2007, the Vung Tau sea monitoring station released data indicates an average increasement of 3.1 mm per year and a total of 9.5 cm rise in sea level from 1979 to 2006 [3]. In late 2019 to early 2020, the Vietnam Disaster Management Authority recorded one of the most heavily impacted sea intrusions in the southeast and the Mekong Delta region. The average of the highest salinity indices measured from 17 stations is 14,100 ppm which is, in reference, 350% higher compared to the last heaviest impacted sea intrusion occurrence in 2016 [4]. As a result, the need for a system that can extract salt from water in Vietnam is rising in order to accommodate the water consumption in agriculture, production and daily routine.

Different concentrations of salt in water are categorized based on their corresponding total dissolved solid values (TDS), as listed in table 3 [5]. For drinking water, no standard is actually specified, however, most drinking water is within the range of 30 – 600 ppm [6]. The quality of drinking water, regarding salt concentration, is highly objective based on the individual's perspective of taste. On a cautionary note, the New York State Department of Health recommends the limit of 20 – 270 ppm for drinking water with patients suffering from cardioactive illness, depending on the severity [7].

Table 2. Water classification based on salt concentration [5].

Type	Total dissolved solid (mg/L or ppm)
Fresh water	< 1,000
Brackish water	1,000 – 10,000
Saline water	10,000 – 35,000
Hypersaline	> 35,000

1.2. Desalination technologies in Vietnam

Desalination is a concept of removing salt ions from saline water to achieve fresh water with a more preferable salt concentration value. Most desalination technologies can be classified as thermal process, membrane process and electrodialysis process.

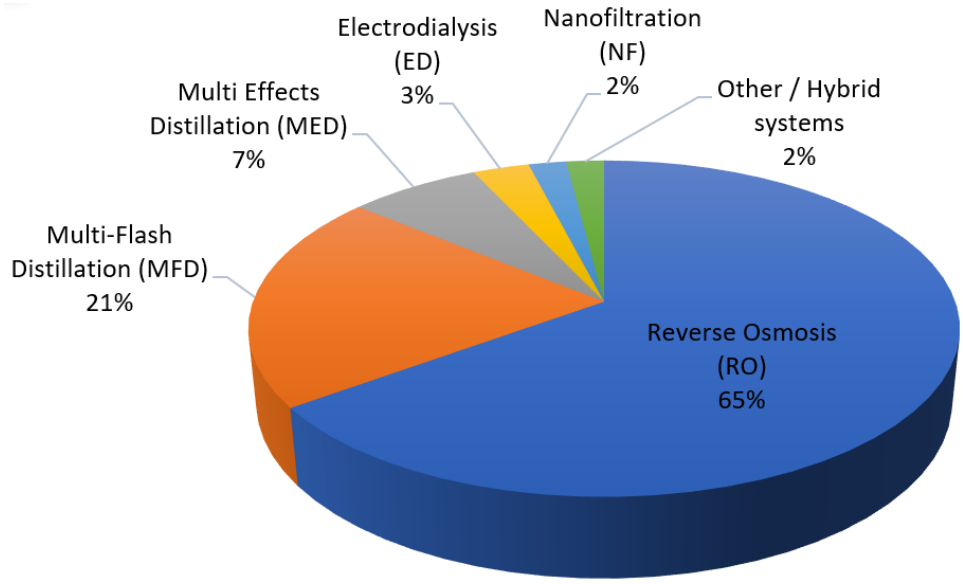

Figure 2. Distribution of desalination technologies worldwide [8].

1.2.1. Thermal process

Distillation is the oldest form of removing impurities from water by using heat to vaporize saline water and then condenses it to produce freshwater. Water is heated to its boiling temperature of 100°C creating water vapor then travel to a pipe system, allowing it to cool down and condense. The resulting product consists of fresh water and the by-product of a high salt-concentration solution called brine. Despite its simplicity, this process holds many disadvantages due to its energy-intensive nature and the fact that this is a relatively expensive solution. Therefore, traditional distillation is usually limited to laboratory and household application.

Derivatives from the traditional distillation such as multistage flash (MSF) distillation, multiple effect distillation (MED), and mechanical vapor compression (MVC) distillation, can achieve higher thermal efficiency by taking advantage of lowering the boiling temperature by reducing its pressure (or vice versa) [9]. Both MSF and MED share a similar concept design of multiple boiling chambers (MSF) or tubes (MED) with decreasing pressure and temperature to partially evaporate seawater. Vapor generated then can be reused as a heating agent for the next chamber/tubes. Meanwhile MVC process, as the name suggested, uses a compressor to increase pressure of the water vapor allowing faster condensation. These derivatives of the distillation process have been existing and widely dominant for decades. However, recent developments indicate that distillation plants will slowly lose its favorability with MSF's contribution to the world desalination capacity decreasing from 78% in 1998 to 21% in 2013 [8].

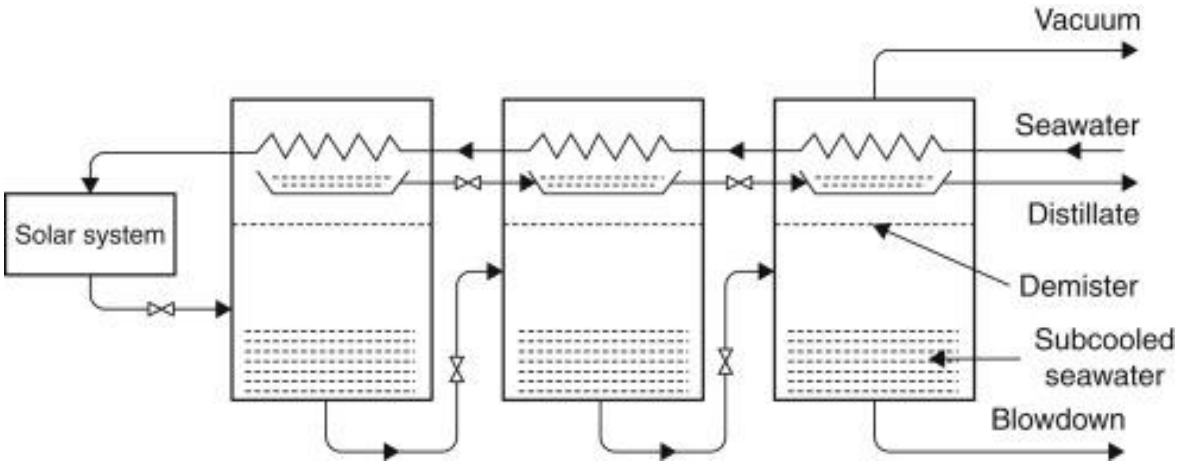

Figure 3. Schematic design of the multi-stage flash distillation (MSF) system [10].

1.2.2. Membrane process

Membrane filtration is a method that removes impurity particles through the use of membranes. Customization of the membrane can be adjusted to match the size of unwanted particles with the four levels of impurity removal are Microfiltration, Ultrafiltration, Nanofiltration, and reverse osmosis (RO). An example of a basic membrane filtration system that can be found in Vietnam is the traditional well digging method. The layers of sand and soil available underground act as a natural filtration medium that removes a certain level of impurities as water passes through.

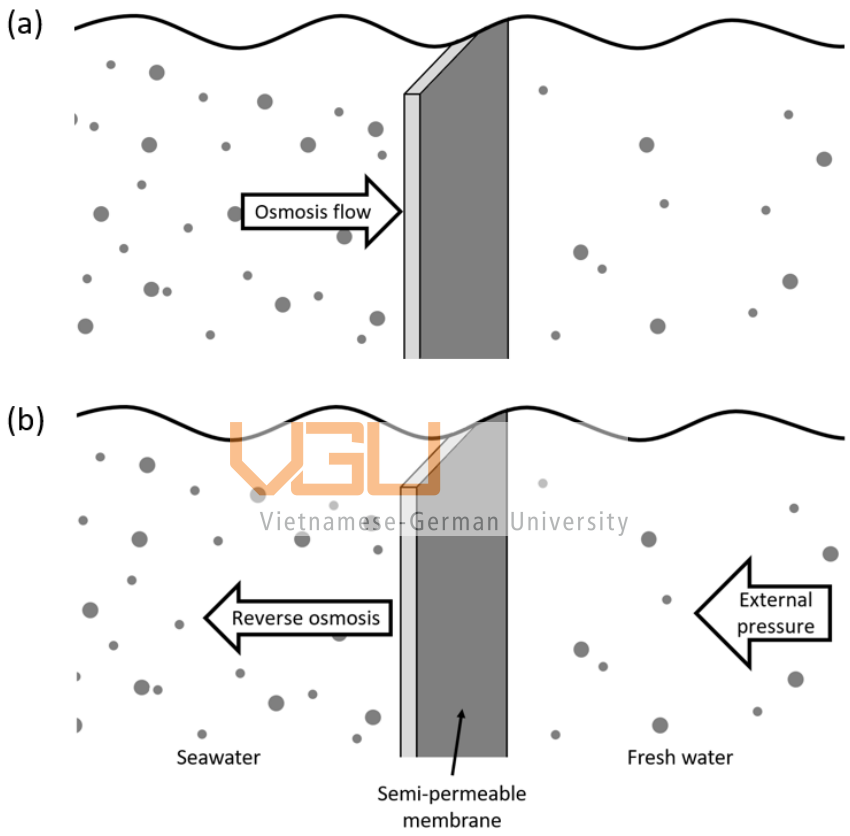

Figure 4. Description of (a) normal osmosis flow and (b) reverse osmosis flow [11].

A more advanced model of this method is the RO system and it can be considered the most efficient and widely used method of water impurity removal. Osmosis flow refers to the phenomenon of fluid movement generated by two liquids with different ions concentration, the solution with lower concentration will have tendency to migrate itself toward the solution with higher concentration [11]. The name reverse osmosis is an indication of the techniques of reversing the natural osmosis flow by administering external force or energy. When combined with the membrane, water is “pushed” through and while water molecules pass through the membrane, impurities cannot. As a result, a high pressure

pump is required to push the feed water through the membrane, higher salt concentration would demand higher force. Despite its overall high removal rate, operation with water under high pressure can lead to design complications with safety risks and immense power consumption. In recent decades, RO is considered the most beneficial method of removing salt, making up 65% of the world's desalination capacity [8]. However, while the RO system can be beneficial in treating high-salt-concentration water, it has proven to be financially unfit when dealing with brackish water [12].

1.2.3. Electrodialysis (ED)

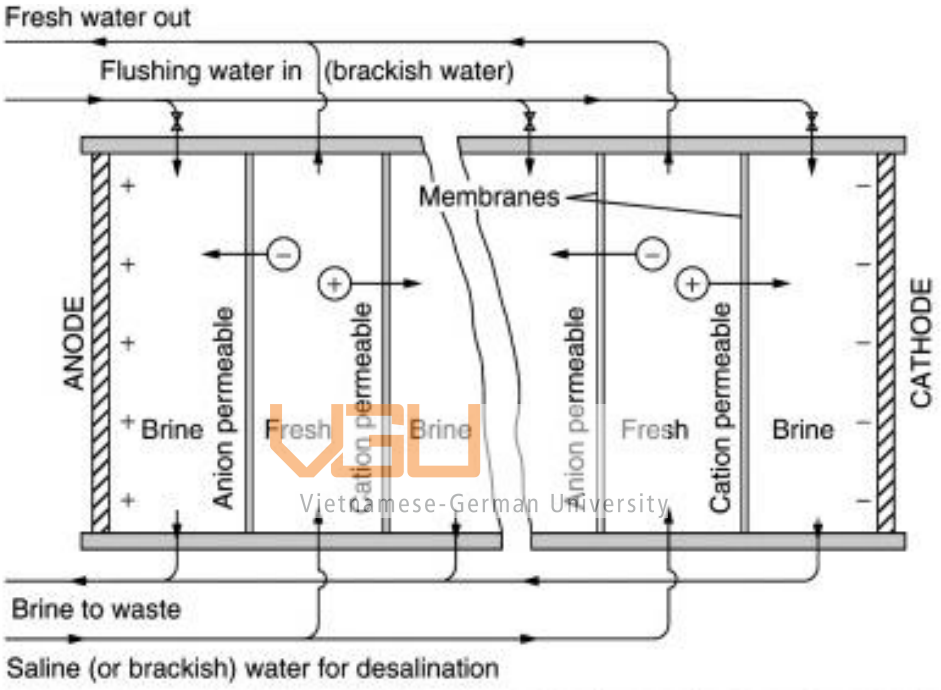

Figure 5. Example of an electrodialysis plant [13].

Contrast to the distillation and membrane process where fresh water is extracted from the seawater, the electrodialysis method removes salt solvents from the water stream instead. The method includes the process of transporting ions from one solution, creating fresh water, to another solution resulting in a high-salt concentration of water (brine). This can be achieved by installing an anion exchange membrane and a cation exchange membrane between two electrodes. The ED process includes generating an electric field across the ED cell to push ion through their corresponding exchange membrane. When apply in industrial use, the electrodialysis cell usually incorporates multiple alternating ion exchange membranes to process water in larger scale [13]. Regarding performance, the ED systems is more beneficial for treatment of brackish water with concentration < 3.000 ppm and for

operations that required higher water recovery rates [14]. In any other cases, i.e., treatment of seawater > 3.000 ppm, the electrodialysis method is much more costly compared to the RO method. Additionally, the ED system is only suitable for removal of charged materials and is proven ineffective when dealing with organic contamination, viruses, etc.

1.2.4. Capacitive deionization (CDI)

Another method of desalination involves the ultilization of potential difference to remove ions from the concentration is the capacitive deionization (CDI) method. Multiple pairs of electrodes fabricated from porous material are stacked together to create a CDI cell with continuous incoming stream of saline water. When apply a voltage difference across the system, salt ions are attracted by their corresponding electrodes and adsorbed into the pore structure of the electrode material. One distinctive feature of the CDI design is the ability to achieve high energy recovery due to its energy storage similar to a capacitor. When combined with the already lower energy required, the balanced energy consumption for CDI operation is significantly lower compared to other processes. For treatment of brackish water, CDI shows promising results with high recovery ratio and energy efficiency. Additionally, since CDI procedure is not heavily dependent on temperature and pressure controls like RO, installation in rural areas with limited resources and manpower is a possibility.

Table 3. Comparison of different desalination methods.

Type	Energy consumed (kWh/m^3)	Operation cost (USD/m^3)
Saltwater Reverse Osmosis (SWRO)	3.0 – 4.0 [15]	0.5 – 1.2 [15]
Brackish water Reverse Osmosis (BWRO)	0.5 – 2.5 [15]	0.2 – 0.4 [15]
Multi-stage Flash Distillation (MSF)	10 – 16 [15]	0.8 – 1.5 [15]
Distillation (MED)	5.5 – 9.0 [15]	0.7 – 1.2 [15]
Capacitive Deionization (CDI)	0.3 – 1.0 [12]	0.07 – 0.4 [12]

2. Literature review

2.1. Experimental and development approaches in recent CDI studies

The concept of capacitive deionization was first introduced in the 1960s by Blair and Murphy [16]. However, it was not until 1996 that the term CDI was officially used to describe the process [17]. Since then, the CDI technologies has gained a great deal of attention as a cost-effective method to remove ions that provide higher water recovery rate compared to the conventional method RO. With more and more research studies emerged in the last two decades. The basic premises of these CDI literature can be categorized into these following topics:

1. Electrode material technologies
2. Operation modes and variations engineering
3. Large scale CDI strategies
4. Targeted removal application

A large proportion of research studies falls under the first category where electrode performance evaluation experiments are conducted by either two approaches: electrochemical (EC) analysis or desalination analysis using a CDI cell. Common electrode material options can include active carbon [18], carbon aerogel [19], carbon nanotube [20], etc. Surface modifications such as using metal oxide coated carbon composites or chemical treatments, can also be applied to enhance the desirable properties. In Vietnam, studies focusing on cost-efficient alternatives for carbon material are also prevalent such as activated carbon electrodes derived from waste coffee grounds [21] and coconut shell [22]. Both studies provide promising results with higher salt adsorption capacity than other conventional activated carbon (table 4).

Aside from electrode technologies, operational design and parameters are also another contributing factor for application of CDI system and its performance. With the introduction of ion exchange membrane (IEM) in 2006 [23], the membrane CDI (MCDI) design overcomes multiple disadvantages that the traditional CDI impose, such as co-ions adsorption and losses due to Faradaic reactions. Additionally, studies regarding several operation modes including constant current (CC) or constant voltage (CV) mode [24, 25], flow-through or flow-by mode [26] and symmetric or asymmetric design [27] provide immersive observation to different design choices.

Table 4. Common base materials for CDI electrode.

Electrode material	Specific capacitance (F / g)	Specific surface area (m^2/g)	Salt adsorption capacity	Ref.
Pure activated carbon	58.29 at 2mV/s	1425	2.82	[28]
Activated carbon cloth	125 at 5mV/s	2794	16	[29]
Mesopore carbon	192 at 1mV/s	1491	0.93	[30]
Hierarchically porous carbon	268.33 at 10mV/s	1058	19.77	[31]
Carbon nanotube	33.36 at 5mV/s	400	23.93	[32]
Carbon aerogel	132.22 at 2mV/s	2523	20.92	[28]
Graphene	160 at 10mV/s	184.19	6.64	[33]
Reduced graphene oxide	140 at 30mV/s	476.7	46.1	[34]

So far, majority of CDI research is often executed in small, laboratory scale with limited attempts to introduce a large-scale design. Due to the nature of CDI operation principles, the system requires stability control as well as treatment procedure to prevents scaling effects on the electrode after long exposure to organic material. One substantial mention is the paper of a continuous operating MCDI plant for the removal of NaCl in biomass hydrolysate [35]. The CDI module construction consist three loops, each loop includes 64 modules of 40 CDI electrode pairs. The resulting arrangement allows production of 1500 m^3/day with operation time of 12.5 h/day. The study suggests to include a 3-minutes 4% HCl wash twice a day as a cleaning procedure to ensure stable production.

Modification of the CDI system can also be implemented to target adsorption of specific ion species. This method is well documented in one study [36], where HNO_3 vapor deposition is used on multi-walled carbon nanotube/poly(vinyl alcohol) composite to favor adsorption of monovalent ions over divalent ions. The approach for this process can be expanded to developed methods of water softening [37], organic matrilateral purification [38] and heavy metal removal [39].

2.2. Theoretical and technical background

2.2.1. Basic designs and operations

A capacitive deionization (CDI) cell, as the name suggests, shares similar design with a capacitor consisting of two electrodes in parallel arrangement. What differentiates the CDI design from a capacitor is the selection of the electrode's components. For desalination purposes, the two electrodes can be separated from each other by either an open air medium or a spacer of mesh-like materials that allows aqueous solution to pass through. Note that the spacer thickness usually would not exceed 500um due to higher resistance created with larger spacers [40]. General properties desired when considering the electrode material are high electrical conductivity, low contact resistance, appropriate wetting behavior, high specific surface area and porous structure. In order for such properties to be satisfied, a variety of carbon-based material and its composites are generally considered as electrode material.

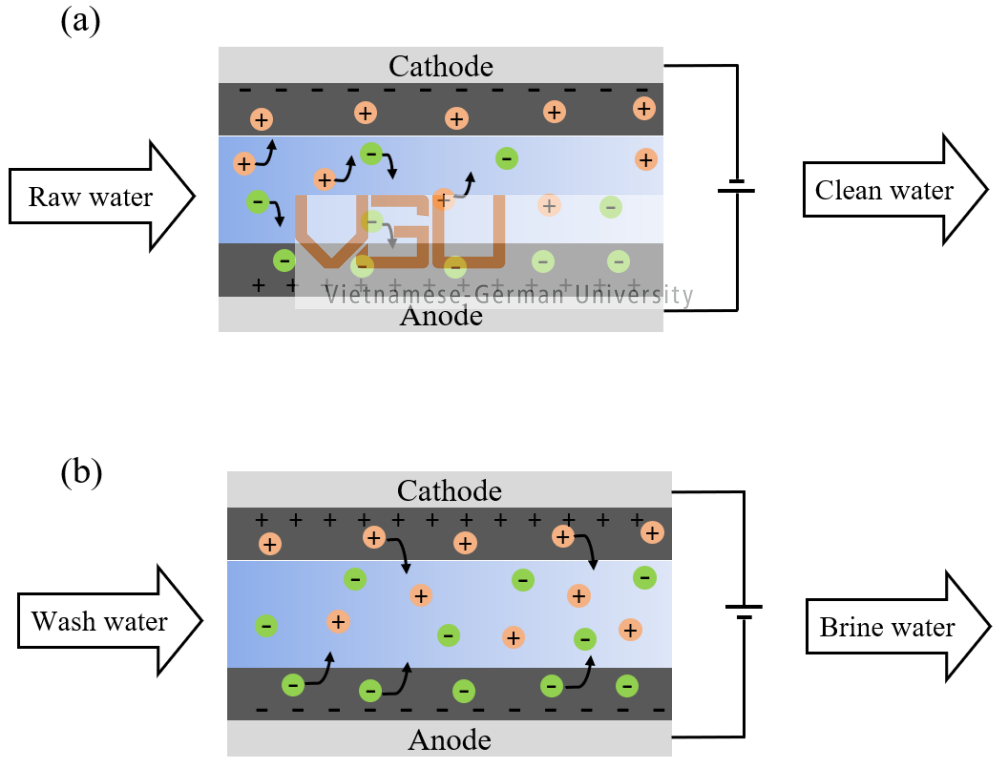

Figure 6. Description of CDI operating principle during (a) charging (absorption) phase and (b) discharging (desorption) phase [41].

The CDI system operates on the principles of electrodialysis which involves the process of ion-exchange under the driving force of an electrical potential. The operation consists of two cycles: absorption and desorption (fig. 6). Absorption begins when a voltage difference is applied between the electrodes creating a charge discrepancy between anode

and cathode. When electrically charged ions in aqueous fluid pass through the system, positive ions (cations) and negative ions (anions) are absorbed respectively by the cathode and anode. The resulting saline solution exits the system with a lower concentration of charge ions.

After some time of operation, the removal rate of the CDI system will decrease. At this point both electrodes are occupied with charged species that were previously removed from the water, this significantly reduces the electronic conductor's surface area which inherently prevents further ion absorption. Reversing the voltage polarity or shorting the circuit would allow the absorbed ions to release itself from the electrodes in high concentration and get discharged by a flow of backwash water. This is referred to as the desorption cycle.

An important observation during the desorption cycle is that the dislodged ions can be reabsorbed by the opposing electrode due to the effect of the reversed electric polarity. This can be considered as a performance loss and non-ideal. A quick-fix for this involves increasing the flow rate of the backwash water feed in order to accommodate the re-absorb rate of the ions. Alternatively, for a more permanent solution, charge-exclusive membranes can be installed in between the electrodes to prevent re-absorption. The membrane acts as a divider that only permits certain ions to pass and not the other (fig. 7).

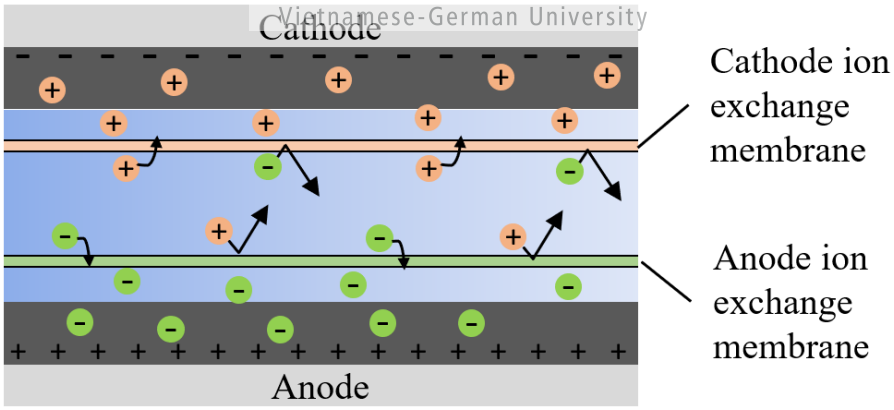

Figure 7. Demonstration of how ion exchange membrane operate [41].

2.2.2. Electrodialysis behaviors in CDI

The core of CDI adsorption behavior with salt ions is expressed through the formation of the electrical double layers (EDLs) on the electrode surface. When the polarized electrode is first in contact with the salt solution, Coulomb's law enforces attraction of counterions and repulsion of co-ions to create the first layer called the Stern layer. The number of adsorbed ions, however, is limited by the electrode surface area as well as the pore structure of the

electrode material. Once the surface area exceeds its adsorption capacity, the total net charge of electrode is still not yet balanced and the remaining electrical potential can further remove ions thus creating the second layer called the diffused layer or the Guy-Chapman layer [42]. For example, in fig. 8a, in the diffused layer, exchanged ions are loosely associated to the electrode via Coulomb force. Along with the anion extracted from the water, additional cations are also pulled toward the anode due to the effect of the negative charge Stern layer and the attraction force from its adjacent counterions. Both the Stern layer and the diffused layer are separated by the Stern plane, while the slipping plane separates the diffused layer and the remaining bulk solution.

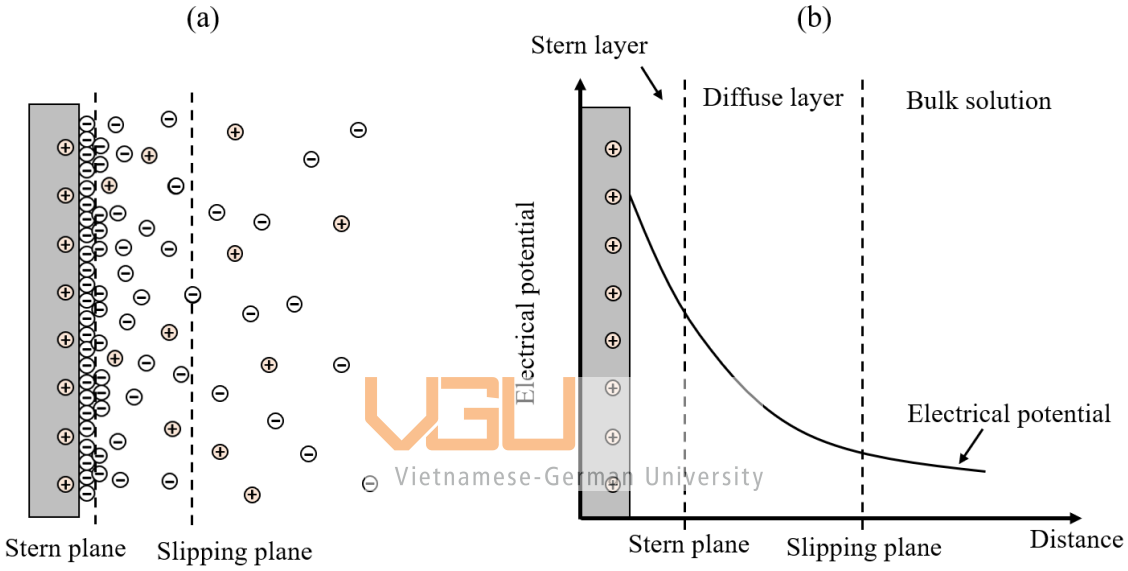

Figure 8. Description of electrical double layers (EDL) formation on one electrode in an infinite fluid body [43].

The Gouy-Chapman model of the EDL formation introduces the relationship of electrode capacitance in terms of applied voltage potential and the ions distribution within the double layers. Observations indicate that the capacitance does not remain constant but instead changes based on the distance from the electrode surface. The observed capacitance consists of two parts, capacitance in the Stern layer and in the diffuse layer, describe as follow [43]:

$$\frac{1}{C} = \frac{1}{C_S} + \frac{1}{C_D} \qquad where \qquad \begin{cases} C_S = \varepsilon_r \varepsilon_0 / r \\ C_D = (2\varepsilon_r \varepsilon_0 F^2 c / RT)^{1/2} \cosh(F\psi_d / 2RT) \end{cases}$$

In which, ε_r is the dielectric constant of the solvent, ε_0 is the permittivity of free space, r is the distance to electrode, c is the monovalent ionic concentration, ψ_d is the Stern potential, F is the Faradaic constant, R is the gas constant and T is the Kelvin temperature.

There are three distinctive electrical potentials that can be measured in the double layers, the surface potential – ψ_0, the Stern potential – ψ_D and the zeta potential – ζ (as in fig. 8b). As the distance from electrode surface increases, potential voltage on the electrode gradually decrease due to the more widely dispersed concentration of ions.

The double layers effects occur in CDI system with two electrode surfaces introduce a slightly more complex EDL model. Firstly, the integration of two opposite polarized electrodes exhibits a shift of the ion adoption capacity between the two electrodes. Because most cations have relatively smaller size than anion [44], given the same electrode surface area, adsorption of positive charge ions would be higher in the Stern layer (fig. 9). Subsequently, the electrical potential of the electrode with higher ion distribution yields higher value. This generates a sense of asymmetry throughout the system where one of the electrodes (usually toward the anode) would perform better than the other one.

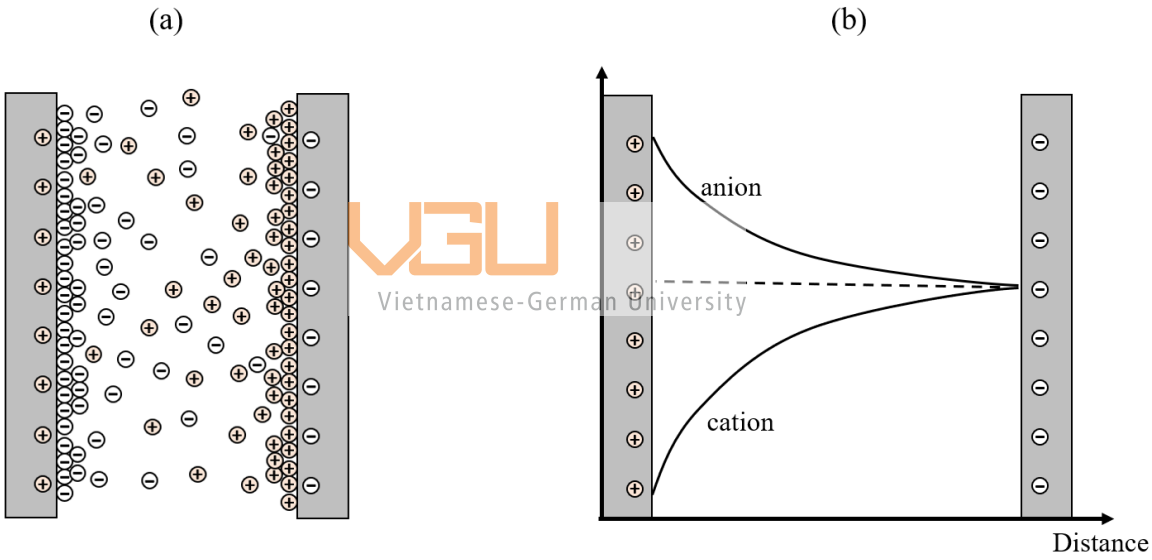

Figure 9. Ions distribution between CDI's electrodes [43].

Additionally, the normal CDI design includes a narrow space between each electrode as wider gaps would increase the electrical resistance of the system. Henceforth when two electrodes with large diffuse layers are facing with each other, overlapping is bound to occurred. The region where two diffuse layers of two electrodes intertwine with each other is referred to as the overlapped diffuse region. This region, however, is non-ideal as it hinders the CDI adsorption performance and is generally recommended to limit as much as possible [45]. As to why this was the case, overlapped regions create alteration of zeta potential value and at the same time changes how ions behave in the double layers. The zeta potential on the slipping plane measures the magnitude of the electrical field that the plane can exert on the

free moving ions in the bulk solution. A high positive value zeta potential (either positive or negative) attracts more counterions and resists electrostatic repulsion caused by adjacent, similarly charged particles.

From the visual comparison between the non-overlapped EDL (fig. 10a) and the overlapped EDL (fig. 10b), the value of zeta potential in the overlapped case became less positive at anode and less negative at cathode. As a result, attraction force exerted on counterions can easily be surpassed by the repulsion force from adjacent similarly charged ions. Strategies to reduce the overlapped region involve methods of optimizing the porous structure of electrode materials by either selecting suitable electrode material or performing surface modifications to achieve desirable results.

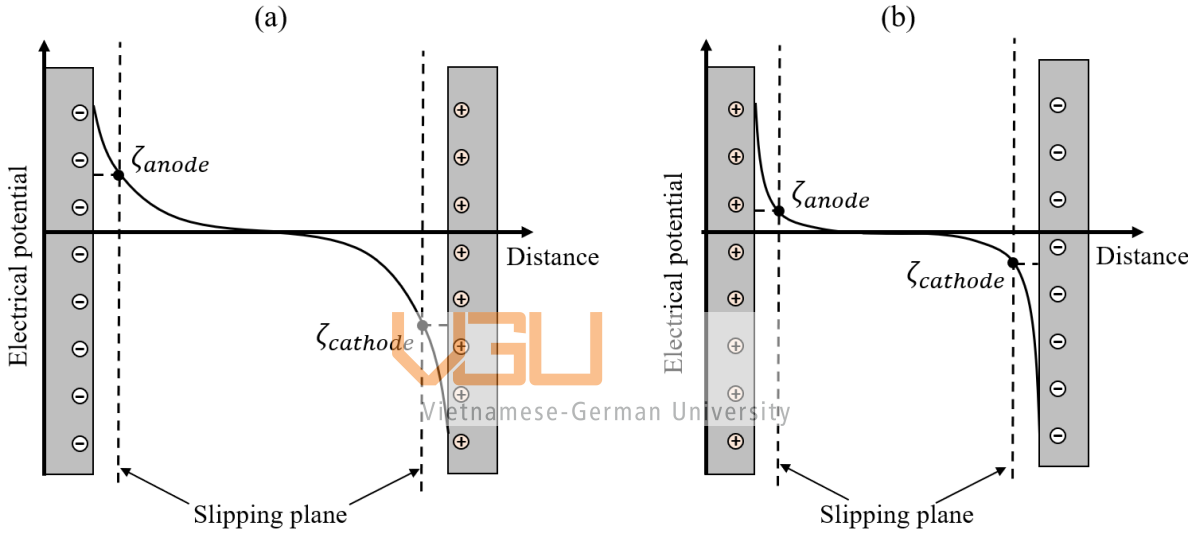

Figure 10. Schematic description of CDI system with (a) non-overlapping EDL and (b) overlapping EDL [43].

2.2.3. Faradaic reactions

During the formation of the EDL when applying a voltage difference across the electrodes, the development of the diffused layer on the porous electrode's surface allows different ions available in the aqueous solution to interact with each other. Typically, this will lead to several chemical reactions between electrode material and water components, also known as Faradaic reactions. Faradaic reactions can either develop at the anode (type I) or cathode (type II) and can occur at a standard electrode potential as low as 0.21V/SHE [46, 47]. Considering the normal CDI operating voltage of 0.6 – 1.2V in most cases, Faradaic reactions are unavoidable, and thus required to be considered during the designing process of the CDI system as they have been proven to interfere with the desalination performance.

Table 8 contains a list of possible Faradaic reactions at both anode and cathode including their corresponding standard electrode potential in volts vs. standard hydrogen electrode (V/SHE).

Table 5. List of possible Faradaic reactions.

Type	Effect	Reaction	
Anode (Type I)	Carbon reduction	$C + H_2O \rightarrow C = O + 2H^+ + 2e^-$	(Eq.1)
		$C + H_2O \rightarrow C - OH + H^+ + e^-$	(Eq.2)
		$C + 2H_2O \rightarrow CO_2 + 4H^+ + 4e^-$	(Eq.3)
	Chlorine oxidation	$2Cl^- \rightarrow Cl_2 + 2e^-$	(Eq.4)
		$Cl_2 + H_2O \rightarrow HClO + H^+ + Cl^-$	(Eq.5)
		$HClO \rightarrow H^+ + ClO^-$	(Eq.6)
		$6HClO + 3H_2O \rightarrow 2ClO_3^- + 4Cl^- + 3/2\, O_2 + 6e^-$	(Eq. 7)
		$Cl^- + 3H_2O \rightarrow ClO_3^- + 6H^+ + 6e^-$	(Eq.8)
	Water oxidation	$2H_2O \rightarrow O_2 + 4H^+ + 4e^-$	(Eq.9)
		$H_2O \rightarrow OH^* + H^+ + e^-$	(Eq.10)
Cathode (type II)	Carbon reduction	$C + H_2O + e^- \rightarrow C - H + OH^-$	(Eq.11)
	Oxygen reduction	$O_2 + 2H^+ + 2e^- \rightarrow H_2O_2$	(Eq.12)
		$H_2O_2 + 2H^+ + 2e^- \rightarrow 2H_2O$	(Eq.13)
		$O_2 + 4H^+ + 4e^- \rightarrow 4H_2O$	(Eq.14)

After prolonged usage, if untreated, Faradaic reactions are capable of causing irreversible damages to the electrode's surfaces. Electrode mass loss and surface deterioration are direct results from the carbon reduction effects (equations 1- 3 and 11). In case of symmetric CDI systems, after time the system will gradually lose their symmetry as the potential voltage difference starts to fall more toward the cathode which furthermore enhances the development of Faradaic behaviors at the positive electrode [48]. Damages to the electrode's surface also subsequently impact the effectiveness of the porous structure (i.e., decrease surface area and/or micropore volume) which ultimately reduce desalination performance. Such performance decline had been recorded in multiple studies; one indicated an average decrease of 50% in salt removal after 50 absorption/desorption cycles [49], while

another demonstrated a significantly lower desalination capacity of 0.5 mg/g at the 70th cycle compared to the initial 4 mg/g capacity [50].

The existence of the Faradaic reactions often results in fluctuating water quality. Particularly, in conventional CDI systems, the water pH levels range between 4 – 10 due to the constant development and consumption of the H+ and OH- ions [51]. Additionally, unwanted presence of chlorate anion (reaction 7) and hydrogen peroxide (reaction 12) accumulated during operation result in sub-standard water output. Concentration of ClO_3^- drinking water is heavily regulated by WHO to not exceed the limit of 0.7 mg/l as they pose significant health risks [6].

Although effects of the Faradaic reactions can sometime be manipulated to achieve desirable features, such as improving desalination performance in some cases [52] and disinfecting water through the generation of hydrogen peroxide, because of its complex nature and multiple unresolved problems that required more investigation it is generally recommended to reduce or eliminate Faradaic effects for an effective overall performance [53]. Preventative methods can include using a membrane CDI system [51, 54]; preferring flow by instead of flow through CDI [26, 55]; favoring constant current operating mode [25]; or optimizing operating voltage window of 0.8V/- 0.4V instead of the traditional 1.2V/0V setup [50]. Alternatively, pretreatment by reducing the oxygen content in water before entering the CDI is also effective in reducing the effect of Faradaic reactions [56].

2.3. Comparison of different types of CDI

2.3.1. Flow-by and flow-through CDI.

Flow mode is one of CDI design components that has a major impact on the system performance, which include the flow-by and flow-through mode. A flow-by design includes a spacer placed in between two electrodes, and within this space, saline solution is then pumped through the system from one end to another, parallel to the electrode surface (fig. 11a). In this structure, the water will interact with both electrodes while salt ions are absorbed into anode and cathode at the same time.

In the flow-through CDI, however, liquid flows from one electrode to the opposite one. The water direction can either be forward (from anode to cathode) or reversed (from cathode to anode), fig.11b illustrates the water movements of the forward flow-through CDI. Due to the high porosity properties of the electrode material, in the case of forward flow-through

mode, as water firstly passes through the anode, salt anions are absorbed into the electrode surface and then move on to the cathode where cations are removed from the water.

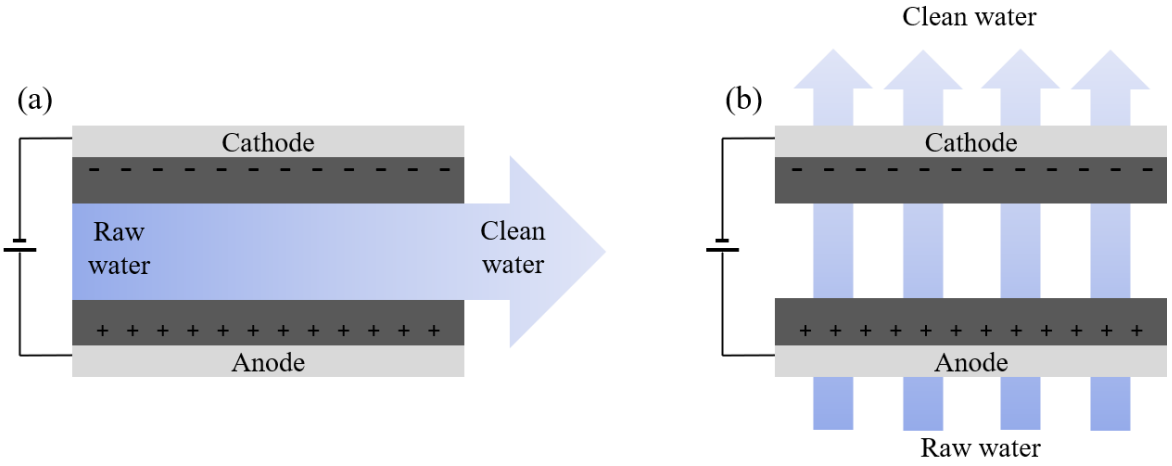

Figure 11. Comparison of different flow mode: (a) flow-by CDI and (b) flow-through CDI [26].

The CDI flow configuration determines how the saline solution would interact with the electrodes. Regarding the flow-through design, water passes through the entire electrode material providing full access to the pore structure for salt ions to be absorbed into. In comparison, the flow-by method indicates fewer interactions since contact between the fluid is restricted only on the electrode's surfaces. Additionally, salt ions removed from the water that are absorbed into the electrode would further limit more ions to be absorbed. Consequently, higher desalination performance is observed in flow-through CDI with the highest efficiency is the flow-through CDI in forward direction given the same electrode mass [34, 55].

However, flow-by CDI can perform better overall in terms of long-term operation and output water stability. One research paper recorded a 77% drop of salt removal rate in flow-through CDI after 120 cycles compared to the 55% drop in the flow-by design [26]. In flow-through operation, as water passes through the first electrode, H+/OH- ions are more likely to be absorbed into the pore structure creating an imbalance of electric charge in the water. Hence, when the water reaches the opposite electrode, Faradaic and non-Faradaic reactions occur more often in order to achieve water electroneutrality. The higher decrease of removal rate in flow-through is a direct result of induced carbon reduction reaction that ultimately leads to electrodes degradation. Higher Faradaic activities also contributes to severe pH changes and high H_2O_2 production [55].

2.3.2. Asymmetric and symmetric CDI

The concept of asymmetry in CDI technologies refers to the differences in configurations between anode and cathode. Those differences can come from the electrode material selection or electrode surface modification method. With the same logic, the term symmetry is used when both electrodes of the CDI are physically and chemically identical.

The option of whether to opt for a symmetric or an asymmetric electrode pair when designing the CDI system depends on how we want to manipulate the potential of zero charge (E_{pzc}) value of each electrode. The E_{pzc} value of a material describes the voltage condition at which the total surface charge of said material to have a net charge equals to zero [57]. Since some material compositions have an unequal number of protons and electrons within their structure, either the insufficient or excess of electrons can cause the electrode net charge to shift to either the positive or negative spectrum. When submerged in an electrolyte solution with no additional electrical potential, the electrode surface will naturally absorb ions in order to achieve electrical neutrality. If the E_{pzc} of the material is higher the decrease short-circuit potential $E_o = 0V$, the electrode at its natural state will have more positive charge ions already absorbed onto the surface. Whereas, with E_{pzc} value lower than E_o, the electrode will have an abundance of pre-absorbed negative charge ions.

Table 6. Potential of zero charge (E_{pzc}) value of some electrode material.

Electrode material	E_{pzc}	Ref.
Carbon aerogel - In 0.01M NaF solution	$0.1\ V$	[58]
Graphene nanopelet - In 50mM PBS solution	$-0.14\ V$	[59]
Activated carbon - In 0.1M KOH solution	$-0.05\ V$	[60]
- In 5mM NaCl solution	$0.605\ V$	[61]

In theory, using identical electrode would yield identical potential of zero charge (E_{pzc}) value for both anode and cathode. During the desorption phase, a positive voltage E^+ is applied to the anode and if the E_{pzc} of anode is larger than E_o, parts of the voltage potential applied contributes to the absorption of counterions, i.e., anions, while the remaining

potential is needed to repel co-ions, i.e., the cations that were already absorbed. Similarly, if the E_{pzc} of cathode is smaller than E_o, part of the potential applied to the cathode is wasted during co-ion repulsion of the pre-absorbed negative charge ions. The usage of identical electrodes consequently leads to the loss of voltage potential in either anode or cathode causing a shift in electrode polarities [27].

For the case of asymmetric CDI, using two different fabrication method for each electrode inherently creating two different E_{pzc} value. Ideally, the E_{pzc} value should be positive for cathode and negative for anode. Since the desalination performance is only restricted by one electrode, the most common way to engineer favorable results is to modify only one electrode. Most common way to alternate material potential of zero charge value is to reduce or increase the surface net charge by introducing impurities to the original electrode material such as p-toluenesulfonate doped polyaniline-activated carbon for the anode [27] or Fluorine doped activated carbon for the cathode [60]. By shifting the E_{pzc} value, the electrodes experience a balanced polarity, i.e., one electrode is not more charged than the other, and achieve more stable desorption after multiple cycle operations.

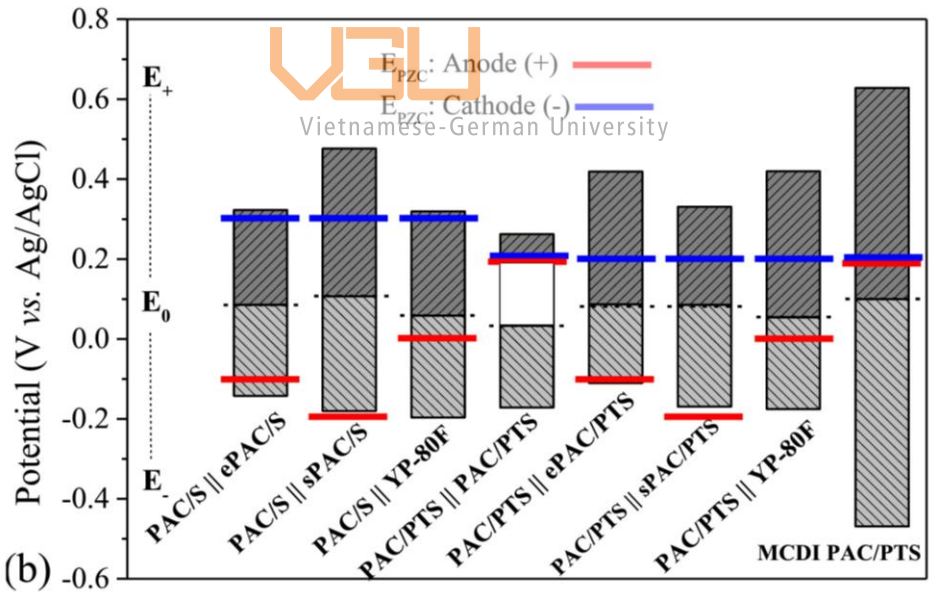

Figure 12. Potential distribution of symmetrical and asymmetrical CDI [27].

Overall, for common desalination usage, it is advisable to use symmetric CDI as most electrode material is electrically neutral and therefore is not chemically selective toward a specific ion species. While successful application of changing E_{pzc} can benefit CDI charge efficiency and overall performance, implementing asymmetry electrode configuration in this scenario would be redundant and ultimately only cause uneven potential distribution [62].

2.3.3. Constant voltage and constant current operation mode

CDI performance can vary with different operating conditions resulting in variances in salt removal rate and energy consumption. Such operation conditions include constant voltage (CV) and constant current (CC) operation mode. CV operation mode involves maintaining a constant voltage difference across the electrodes, preferably from 1.2V - 1.5V to avoid Faradaic and hydrolysis reactions. During the discharging phase, reverse the CDI polarity or simply create a short circuit by connecting the poles together in order to remove the adsorbed salt ion. Consequently, the current behavior in CV mode, similar to how current conducts in a capacitor, would initially start at a specific value and slowly decrease until it reaches zero. The charging and discharging time period are determined based on how long it took for the current to drop from its initial value to zero (fig. 13a, b).

On the other hand, in CC mode, constant current is applied to the electrode during the charging phase and either a reverse current or a current of 0A for the discharge phase. Throughout the charging period, voltage value would increase with the constant current and then finally drop to zero when the current is reversed. In order to accommodate the voltage recommendation, the charging period is designed to end when the voltage reaches 1.2V (fig. 13c, d).

In general, most CDI systems preferably operate using CV mode due to its easy controllability of voltage level and higher removal efficiency of the same absorption time [24, 25, 63]. Nonetheless, operation during CC mode yields a more stable and constant conductivity level, allowing simple control over the output water conditions. Regarding energy consumption, constant current operation mode is proven to achieve more effective energy performance in both the overall total energy consumed and the amount of energy required per milligram of salt removed [24, 25]. Hence, it should be kept in mind either to compromise energy efficiency for higher desalination or vice versa when it comes to choosing between CV and CC method.

Alternatively, another operation mode was introduced in one research paper that instead of sustaining constant voltage like in the traditional CV method, voltage increases in stages with the number of stages can vary from two to eight stages. Observation suggests that the more steps (or stages) there are, the more resemblance that the step voltage (SV) mode has compared to the CC mode in terms of removal rate and energy efficiency. The 2-stages SV operation mode, which involves applying constant voltage of 0.5V for the first

half of the charging period and increasing to 1.0V for the final half, provides a middle-ground option with higher power efficiency than the CV method and higher removal performance than the CC method [63].

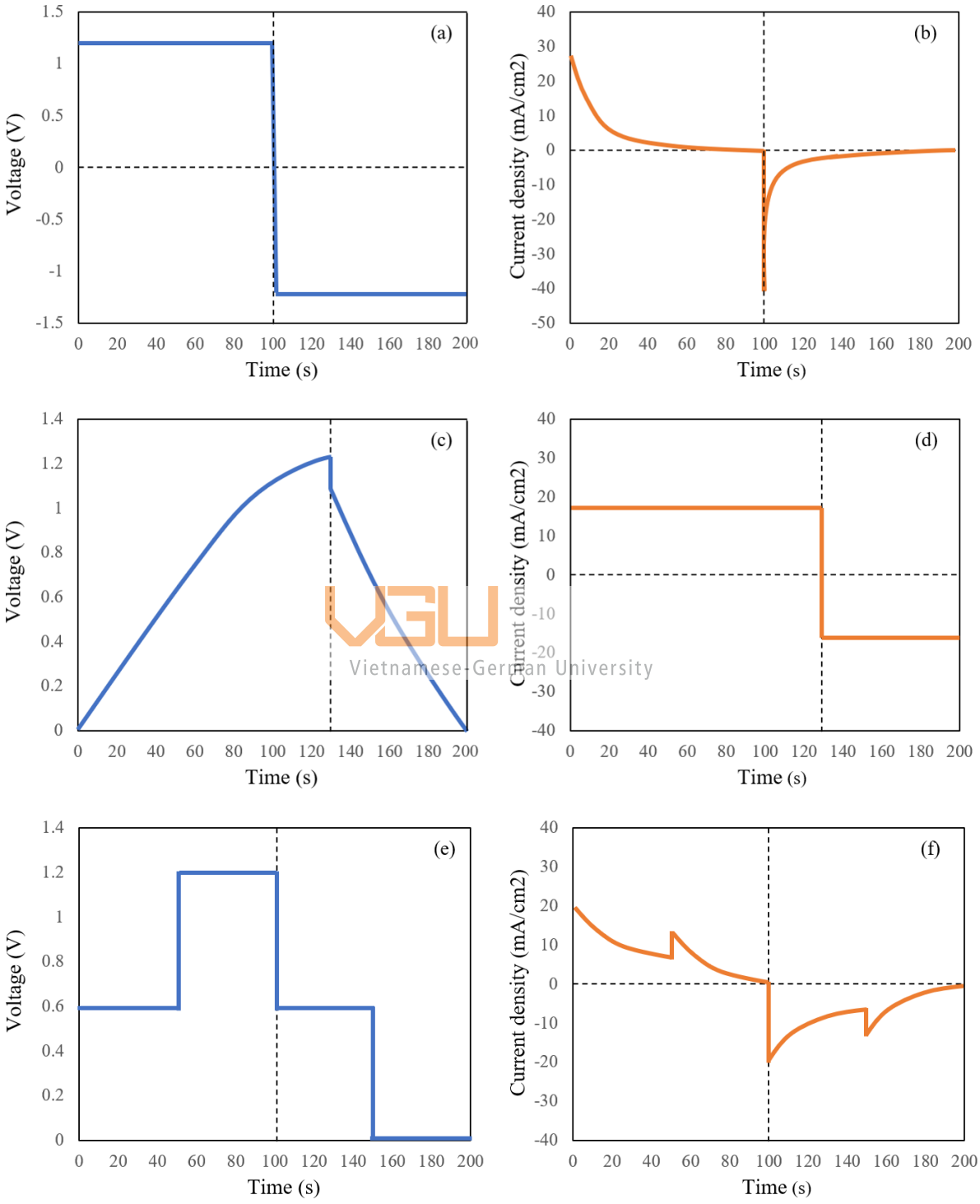

Figure 13. Comparison of: voltage (a) and current (b) of CV mode; voltage and current (d) of CC mode; voltage (e) and current (f) of SV mode [25, 63].

2.4. Electrode technology

2.4.1. The science of electrode porosity on desalination performance

As previously mentioned, the selection of electrode material can greatly impact how efficient the CDI system can perform. The porous structure of said material plays a vital role in determining the absorption behaviors of salt ions. According to traditional electric double layer (EDL) theorem, the majority of absorption activities are favored in the mesopores region in which the pore's diameter ranges between 2-50 nm. From most studies [64], we can distinguish a trend of increasing desalination performance accompanied with increasing pore size and pore distribution per unit area while still adhering within the mesopore limit. Understanding of the conventional EDL theories allows us to explain this phenomenon through the mechanism of electrosorption within the overlapping diffuse region. The double layer overlap effect existing in the overlapping region abides desalination activity, henceforth larger pores that allow easy access for ions to occupy in that empty space would increase the quantity of ions in the Stern layer and ultimately contribute to the reduction of electrical double layer overlapping.

However, it should be kept in mind that larger pore size would subsequently lead to lower overall surface area which is a performance-limiting factor. Additionally, although smaller size mesopores are more efficient removing salt they can be more costly due to their high energy expense. One research paper recommended that medium size pore of approximately 5nm would be the most balanced option with good salt removal rate and reasonable energy consumption [64-66]. For comparison, table 1 includes a list of commonly used unmodified electrode material accompanied with their corresponding structure properties.

In spite of the fact that most of electro-absorption occurs in mesopores, it is necessary to point out that the impact of microporosity (pore width < 2nm) on the desalination performance might still be worth considering as most electrode materials are mostly dominated by micropores (see table 1). One recent study has suggested a higher electro-absorption density in micropore while evaluating different models of activated carbon cloth with various micropore/mesopore ratios [67]. It has been brought to light that absorption at micropore operates with different mechanisms compared to mesopore. Introduction to modern EDL theorem was provided with more sophisticated models that consider ion dehydration and water – water interactions which was previously missing from the classical

EDL studies. In contrast to traditional theories, ions were described to form a single layer at the middle of the split-like pores. On the other hand, in that same study, it is important to note that increasing the micro-to-meso ratio would promote the ion selectivity behavior. This is especially prevalent in higher micro/meso material as absorption in micropore is more restricted to salt ions with higher hydrated radius (table 2).

Depending on usage, either to selectively remove unwanted substances in fluid or salt removal for general purpose, the micro/meso ratio can be adjusted to optimize electrosorption capacity for both mechanisms. Furthermore, in spite of the fact that some general rules regarding selecting electrode material based on its pore structure, due to the complex nature of different sorption methods and multiple contribution variables such as water concentration, ion size, etc., case-by-case study and experiment is highly recommended when designing efficient system [64, 67].

Table 7. Characteristic of commonly found salt ions.

Ions	Hydrated radius (nm)	Ions	Hydrated radius (nm)
Na^+	0.358 [68]	F^-	0.352 [69]
K^+	0.331 [68]	Cl^-	0.332 [69]
Mg^{2+}	0.428 [68]	ClO_4^-	0.395 [69]
Ca^{2+}	0.412 [68]	NO_3^-	0.334 [68]
Fe^{2+}	0.430 [70]	PO_4^{3-}	0.339 [71]
Fe^{3+}	0.480 [70]	SO_4^{2-}	0.300 [71]

2.4.2. Surface modification methods for improving electrode properties

In general, modifications of carbon-based electrodes usually can be done either through chemical treatment or metal oxide coating. Chemical treatment process involves submerging the carbon material in a liquid for a specific amount of time while maintaining the solution's temperature. The most prime examples of chemical usage in this approach are nitric acid [72, 73], sulfuric acid [74], sodium hypochlorite, potassium permanganate [75], etc. Regardless of the method, the main goal of surface modification is to manipulate and achieve favorable porosity and electrical properties of electrodes.

Method of disposition of metal oxide can varies such as applying a thin metal oxide film with adhesive [76] or combining the oxide powder with the original material to create a slurry mixture that later used to cast the electrode [77]. By introducing foreign molecules, the atomic structure can be altered to engineer specific micropore/mesopore ratio or increase surface area. Success applications of metal coat (table 6) exhibit great improvements onto the electrode surface and higher desalination performance. One limitation of using metal oxide coats is that during prolonged usage, this metal oxide residue might detach itself from the electrode due to breakage and is then released into the water flow.

Impact of chemical treatment on the surface structure varies from case to case depending on the selection of chemical used and the base material. In the case of nitric acid treatment on activated carbon, it can be observed that the pore structure of sure evolves from various micropores with average size of 10um to larger merged mesopores accompanied with noticeable decrease in specific surface area [73]. On the other hand, chemical treatment can also be administered to decrease the pore size to accommodate the suggested value of 5nm for balance between desalination rate and energy consumption. Evidence supporting the statement is prevalent in these studies evaluating sulfuric acid treated activated carbon [74] and multiple different treatments on carbon nanotubes [75]. Surface modification through chemical treatment allows control over the treatment period of which material is submerged in the oxidizing liquid. The degree of differential from the original value subsequently increases as exposition to chemicals are extended [77].

Table 8. Comparison of different metal oxide coating surface modification.

Electrode material	**Specific capacitance (F / g)**	**Specific surface area (m^3/g)**	**Desalination capacity (mg/g)**	**Ref.**
Graphene (rGO)	160 at 10mV/s	184.19	6.64	[33]
Graphene/20% TiO_2 composite (rGO/20%TiO_2)	325.8 at 10mV/s	382.08	8.52	
Activated carbon cloth (ACC)	80.0 at 5mV/s	655.1	12.9	[78]
Activated carbon cloth/graphene oxide composite (ACC/GO)	86.1 at 5mV/s	744	16.7	

Activated carbon (AC)	182.33 at 2mV/s	415.61	n.a	[79]
Activated carbon/MnO_2 composite (AC@MnO_2)	335.6 at 2mV/s	324.2	25.7	

2.4.2.1. Enhancing electrical capacitance

Due to its physical attributes, carbon-based electrodes are usually limited in capacitance with the maximum value not exceeding 300 F/g for most materials (table 6,7) and 150 F/g for activated carbon [40]. Increasing this value by using oxide of transition metals with higher capacitance capability is one of the most effective methods to enhance the overall performance of the CDI system. Common oxides that are often chosen by this method are similar to those used when designing supercapacitors such as magnesium dioxide MnO_2, titanium dioxide TiO_2, copper (II) oxide CuO, iron (III) oxide Fe_2O_3, etc.

Table 9. Comparison of different chemical treatment surface modification.

Electrode material	**Specific capacitance (F / g)**	**Specific surface area (m^3/g)**	**Desalination capacity (mg/g)**	**Ref.**
Activated carbon (AC)	106.6 at 5mV/s	1295	0.56	[73]
Nitric acid treated activated carbon (NTAC)	381.7 at 5mV/s	747	0.85	
Activated carbon (AC)	219 at 1mV/s	1477.2	2.68	[74]
Sulfuric acid treated activated carbon (FAC)	232 at 1mV/s	1244.7	3.54	
CO2 treated Novolac-derived carbon beads (PNC-CO2)	124	2317	8	[80]
H2 treated Novolac-derived carbon beads (PNC-H2)	127	2193	11.5	

2.5. CDI in industrial scale application

2.5.1. Stacking effect of scale up CDI system

Scale up is a technique to design a CDI system with larger adsorption capacitance based on a pilot scale design. One of the many ways to achieve larger water capacity is the stacking method which involves connecting multiple CDI units to process simultaneously. Because CDI, in basic terms, is considered a capacitor, each CDI unit can be connected in either series or parallel configuration (fig. 14).

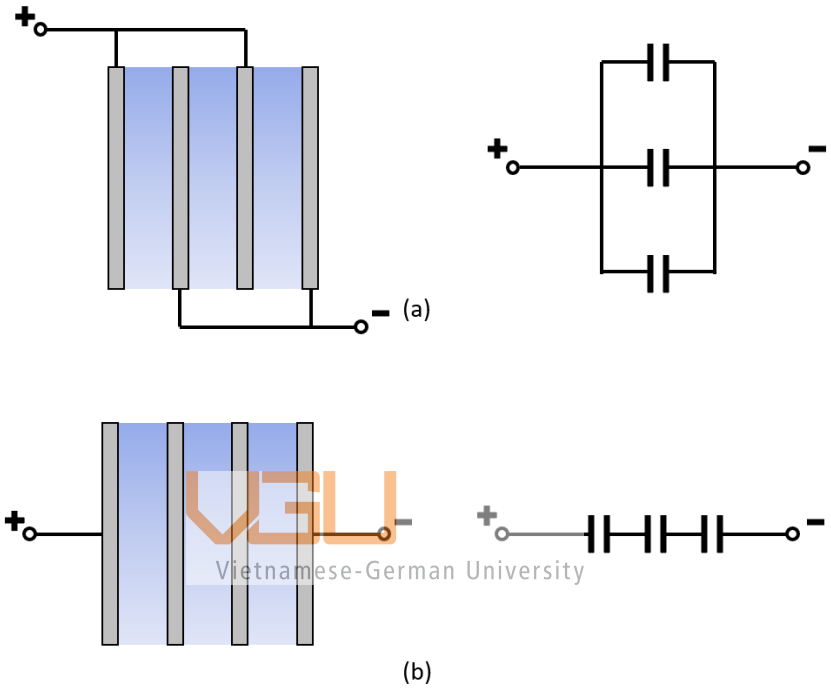

Figure 14. Description of electrical equivalent of (a) parallel stacking CDI and (b) series stacking CDI [81].

The parallel configuration involves connecting every anode and cathode to the positive and negative terminals of the power supply respectively. Thus, each electrode pairs in the parallel configuration are applied with the same voltage potential. Operations with parallel stack CDI usually include low voltage potential, however, in order to compensate for the number of CDI units, high current must be provided. This can cause complications when controlling a low-voltage and high-current power supply.

On the other hand, the series connection requires only the outermost electrodes to be connected to the power supply. The resulting CDI system will have the same charge current flow through each CDI unit. The voltage potential of the in between electrodes will be induced despite being in contact with the power supply terminals because of the electrical

field mechanism. Compared to the parallel configuration, the series-CDI operates with a high-voltage and low-current power source.

Despite the simple design, the series stack CDI is much less electrically efficient, especially with a higher number of CDI pairs [81]. Majority of electrical resistance within the CDI unit is caused by salt solution, therefore, when connected in series, loss due to resistance is more prevalent. Because applied voltage is only controlled at the outermost electrodes, electrical loss creates uneven potential distribution at the in between electrodes and decreases performance of those electrodes. Although, parallel configuration requires more advanced design to allow voltage potential control of each and every electrode, it effectively incorporates the usage of multiple CDI units without substantial loss.

2.5.2. Single-pass mode and batch mode for CDI analysis

Before a CDI design is applied to a system, evaluation of desalination performance must be performed by measuring the water concentration variance and the amount of salt absorbed with time. Conductivity of the solution can be evaluated in two different methods: the single-pass mode or the batch mode. Depending on the analysis method, behaviors of solution conductivity will differ throughout the process.

In the single-pass mode, raw water is pumped into the system from one container and after treatment will exit the system to a different container (fig. 15a). A conductivity probe meter is placed at the output reservoir to measure the water quality. At the beginning of the desalination process, the conductivity value of the water drastically decreases to its minimum value. As the electrodes reach their capacity, the water concentration slowly increases again until it regains its initial value (fig. 15b).

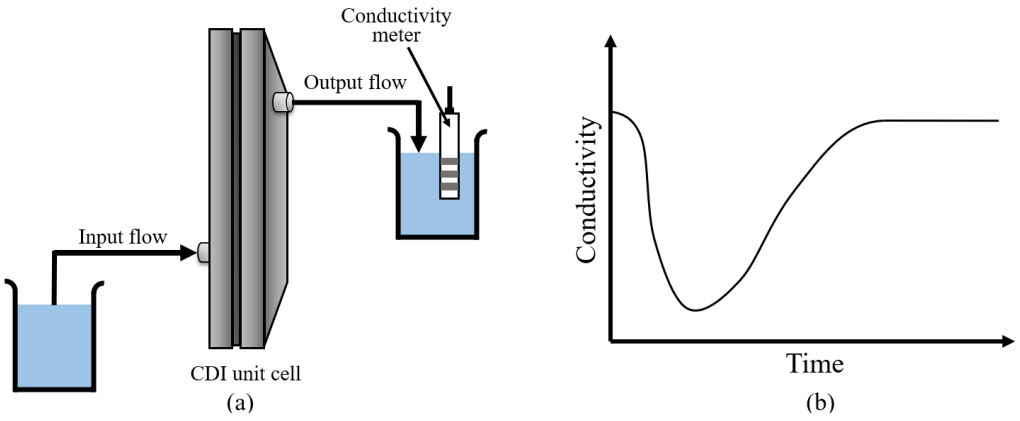

Figure 15. Description of (a) single-pass mode operation and (b) effluent conductivity value vs. time in single-pass mode [41].

In batch mode operation, however, salt water cycles through the system multiple times by using only one reservoir for the system (fig. 16a). This reservoir will be the measure point to evaluate the conductivity value. Instead of having a minimum concentration point as in single-pass mode, the conductivity in batch mode steadily decreases its value until its levels off (fig. 16b).

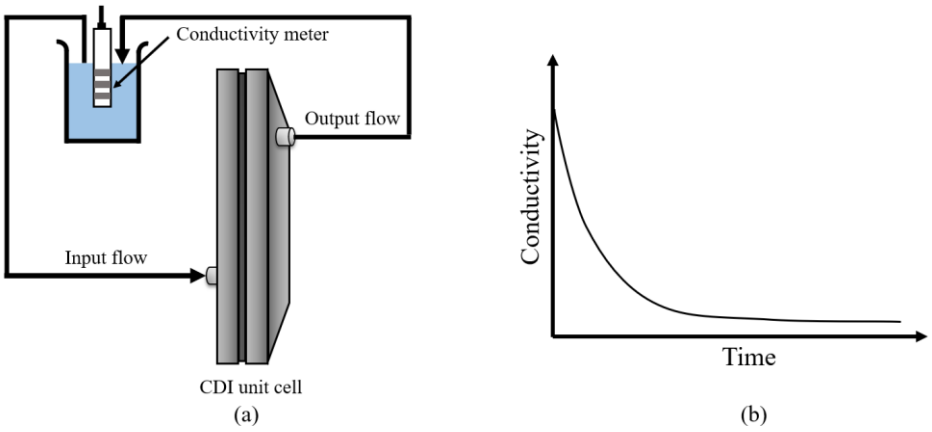

Figure 16. Description of (a) batch mode operation and (b) effluent conductivity value vs. time in batch mode [41].

When compared, both the single-pass mode and batch mode are capable of determining the total salt adsorption capacity (SAC) of the electrode as follow [41]:

$$SAC_{single} = \int_{t_{desalinate}}^{0} VC(t)dt$$

$$SAC_{batch} = (C_o - C_e) \times V$$

In which, V is the volumetric flow rate (L/min), $C(t)$ is the effluent concentration (mg/L) with C_o is the initial concentration and C_e is the equilibrium concentration. Desalination performance of the system is determined through the feed water initial salinity, desalination flow rate and the voltage potential. However, the batch mode operation exhibits limited analysis because salt absorption behavior is also dependent on another parameter, the volume of the reservoir tank. This additional variable ultimately makes it difficult to compare results of different CDI experiment designs [41].

3. Methodology

3.1. CDI cell preparation

Both anode and cathode electrodes are synthesized using Siontech (Korea) carbon-based mono electrode sheets. Each electrode sheet consists of a graphite sheet with activated carbon (P-60, Kuraray Chemical Co., Japan) distributed on each side of the sheet. The graphite sheet acted as a conducting material to apply voltage across the carbon electrode. Dimensions of the carbon electrode are 70mm x 70mm with body mass of 0.5g per pair of electrodes.

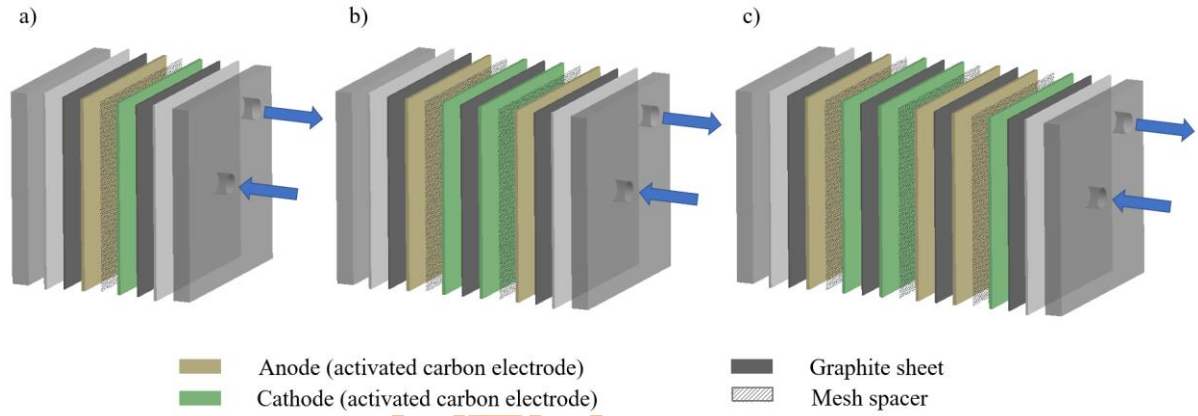

Figure 17. Assembly representation of a CDI unit cell with (a) one pair of electrodes, (b) two pairs of electrodes and three pairs of electrodes.

The electrode pair assembly includes two graphite sheets. A polymer mesh space of thickness 200um is placed between each anode/cathode pair, separating the electrodes and allowing fluid motion across the system. Additional electrode pairs can be stacked parallel with alternating polarity. Because the activated carbon can be distributed on either side of the graphite sheet, each electrode pair will have at least one co-joining graphite sheet (fig. 17). This paper will focus on the analysis of CDI unit cells with one, two and three pairs of electrodes, denoted as CDI-1, CDI-2 and CDI-3, respectively. Specification of CDI cells provided by the manufacturer are included in table 10.

Table 10. Specification of experiment CDI cells.

	CDI-1	**CDI-2**	**CDI-3**
Spacer volume (mL)	2	4	6
Capacitance (F)	198.6	279.9	397.2
Total surface area (m^2)	2703.2	4054.8	5406.4

3.2. Feedwater preparation

In this paper, only solution of single salt concentration will be used to evaluate CDI perform. Because of this, the experiment is limited to desalination under ideal water condition with few to none organic contamination. Actual results from real life application of seawater with complex composition may slightly varies from the final outcome of this paper. The decision to use single salt concentration allows in-time observation and measurement of output effluent concentration of the system and therefore provide direct conclusion to how different operation specification effects the CDI performance.

Feedwater during both the adsorption and desorption phase is prepared with deionized water and laboratory grade NaCl (Xilong Scientific Co., Ltd, China). Different concentration of the solution is adjusted to achieved desired TDS value ranges from 200 ppm to 1000 ppm.

3.3. Equipment setup

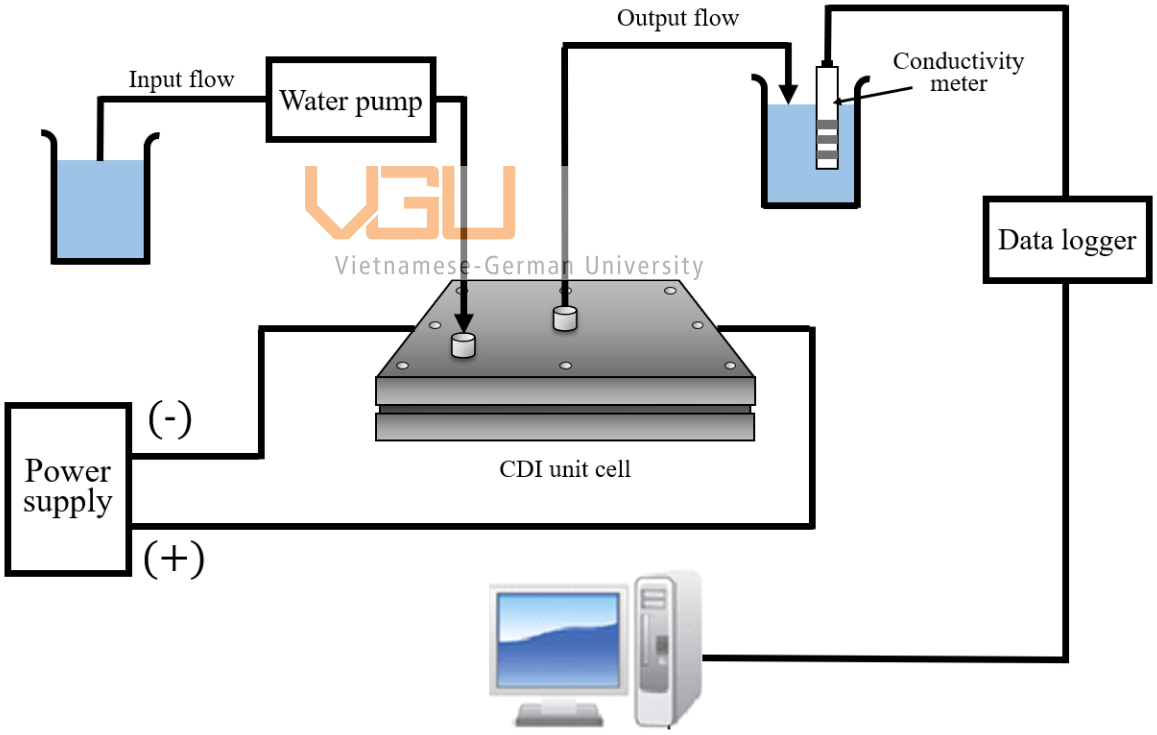

Figure 18. Description of CDI analysis experiment set up.

Fig. 18 describes the laboratorial setup of the CDI experiment. All three CDI units (CDI-1, CDI-2 and CDI-3) are single pass system with the infeed water is prepared from deionized water with different concentration of NaCl. An adjustable DC regulated power source (HDS1500PS12, XP Power, Singapore) is connected directly to the CDI electrodes while a pump () simultaneously pumping saline solution through the system. Outgoing water

exits the CDI and passes through a conductivity meter rod (HORIBA, Japan) with a data logger where all data is collected and further analyzed through MATLAB. The whole system is then automated using a simple Arduino program from a computer to control CDI charging and discharging time.

3.4. Experiment description

All experiment conducted in this paper is executed in single pass mode with a constant voltage applied across the system. The adsorption and desorption cycle time are fixed to maintain constant water recovery rate of 66.7%. Each experiment focuses on the how the CDI system performs under different operating conditions, including:

1. Various initial concentration of feed water: 200/400/600/800/1000 mg/L.
2. Various applied potential difference: 1.0/1.1/1.2/1.3/1.4 V.
3. Various feed water flow rate: 400/600/800/1000/1200 mL/min.
4. Different configurations of discharging mode: 150s of RVD, 50s of ZVD followed by 100s of RVD, 75s of ZVD followed by 75s of RVD and 100s of ZVD followed by 50s of RVD.

These four configurations are applied to all three CDI cells (CDI-1, CDI-2 and CDI-3) in order to make straight-forward comparison. In total, we have 57 samples, each sample is then repeated three times and the final values is taken by averaging the observed results.

3.5. Performance parameter

Considering the nature of this experiment is to evaluate performance of the CDI units with different operating variable, it is important to establish quantitative performance metrics

3.5.1. Water quality

The output water quality of the CDI can be evaluated through multiple indicators. Firstly, we consider the concentration reduction, i.e., the total mass of salt removed from the solution. The concentration reduction is defined as follow [82]:

$$\Delta N_C = \int_{\Delta t_c} Q\left(C_{feed} - C_{out}\right)dt \qquad \text{(Eq. 15)}$$

where Δt_c is the charging phase period, Q is the infeed flow rate and C_{feed}, C_{out} are the fluid concentration measured at the input and output of the system. The water concentration units are often (mg/L) or equivalently (ppm).

Another parameter that are often used when evaluating CDI performances is the salt removal rate, which are defined as follow [82]:

$$removal\ rate = \frac{\Delta N_C}{QC_{feed\Delta t_c}} \quad \text{(Eq. 16)}$$

A typical household CDI model usually have removal rate ranges from 60% - 80%. However, with this pilot model, we expect the system to have a much lower removal efficiency due to its small size.

3.5.2. Energy efficiency

The equation for total energy consumption of the CDI unit during charging or discharging operation is described below [82]:

$$E_{tot} = \int IVdt \quad \text{(Eq. 17)}$$

Equation (17) can be applied for either constant current or constant voltage mode. For better analysis, volumetric and specific energy requirement can

$$E_v = \frac{E_{tot}}{V_c} = \frac{E_{tot}}{Q\Delta t_c} \quad \text{(Eq. 18)}$$

$$E_m = \frac{E_{tot}}{\Delta N_c} \quad \text{(Eq. 19)}$$

Where E_v is the energy consumed to generate one unit of fresh water (kJ/L) and E_m is the energy needed to removed one unit of salt mass (kJ/g).

3.5.3. Electrode regeneration rate

After each adsorption cycle, the adsorbed ions must be removed from the CDI electrode in order to maintain stable operation for the next cycle. During this process, incomplete regeneration of the electrodes leads to decrease of desalination efficiency and lowers the output water quality. The regeneration rate (%) is defined as follow [82]:

$$regeneration = \frac{\Delta N_d}{\Delta N_C} = \frac{\int_{\Delta t_d} Q_c(C_{feed} - C_{out})dt}{\int_{\Delta t_c} Q_c(C_{feed} - C_{out})dt} \quad \text{(Eq. 20)}$$

Where ΔN_c is the amount of salt removed from solution during adsorption phase and ΔN_d is the amount of salt released from the electrode back to the water.

4. Results

4.1. Effects of various infeed concentration on desalination performance

4.1.1. Experiment data

Salt solution with varying concentrations from 200 to 1000mg/L, at a constant flow rate of 400 mL/min and applied voltage difference of 1.2V are used to evaluate the performance of the CDI-1 system. Fig. 19 illustrates the water concentration of different systems throughout the adsorption and desorption phase. Observation indicates faster desalination activity with decreasing feed TDS as the salinity value's inclination is susceptible to the electrical resistance of the solution. With lower TDS value, the solution ability to conduct electricity decreases due to the lack of moving ions which inherently leads to quicker current depletion (fig. 20). This reasoning can also be applicable to the stacking effects on desalination performance of the same initial concentration. In the case of CDI systems with two and three pairs of electrodes, each pair is connected parallelly and therefore the internal resistance as a whole is smaller than that in system with one pair. The lowest concentration achieved by the double pairs system, compared to the single pair CDI, is approximately 1.5 times lower while the triple pairs system is 2 times lower.

Regarding desorption performance, the model exhibit trends of increasing amount of salt mass removed from the liquid with increasing concentration of input fluid, as depicted from fig. 21a. Lower electrical resistance from higher saline water allow more ions exchange between the two electrodes with the highest amount of 23.6 mg of NaCl removed at 600 ppm and the lowest of 19.7 mg at 400 ppm. On the other hand, while the total amount of salt increases, the salt removal rate behaved inversely. This is because of the electro-adsorption capacity within the CDI are heavily limited by the surface area of the electrode, i.e., the total electrode mass. In order to achieve higher removal rate for higher TDS concentration more available pores would be required. This is further supported by the fact that desalination of multiple electrode pairs CDI of the same initial TDS has higher removal rate because there is more electrode surface area. Result shows varying desalination rates from 1.5% to 2.7% for the CDI-1 system while removal rate from 1.7% - 4.3% and 2.3% - 5.8% for CDI-2 and CDI-3 respectively (fig. 21b).

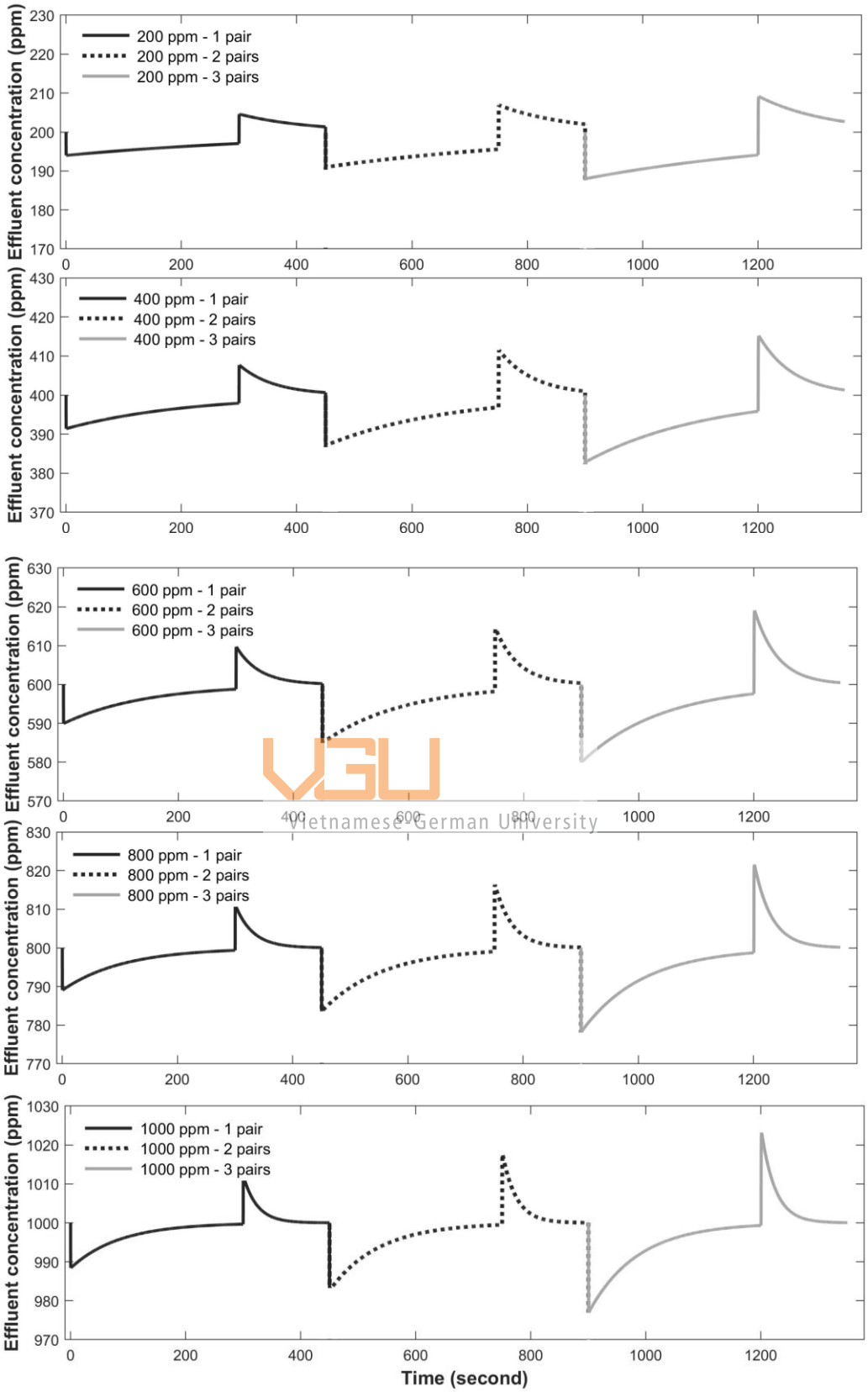

Figure 19. Effluent concentration at exit for different TDS feed water (Flow rate: 400mL/min; applied voltage: 1.2V; WR 66.7%).

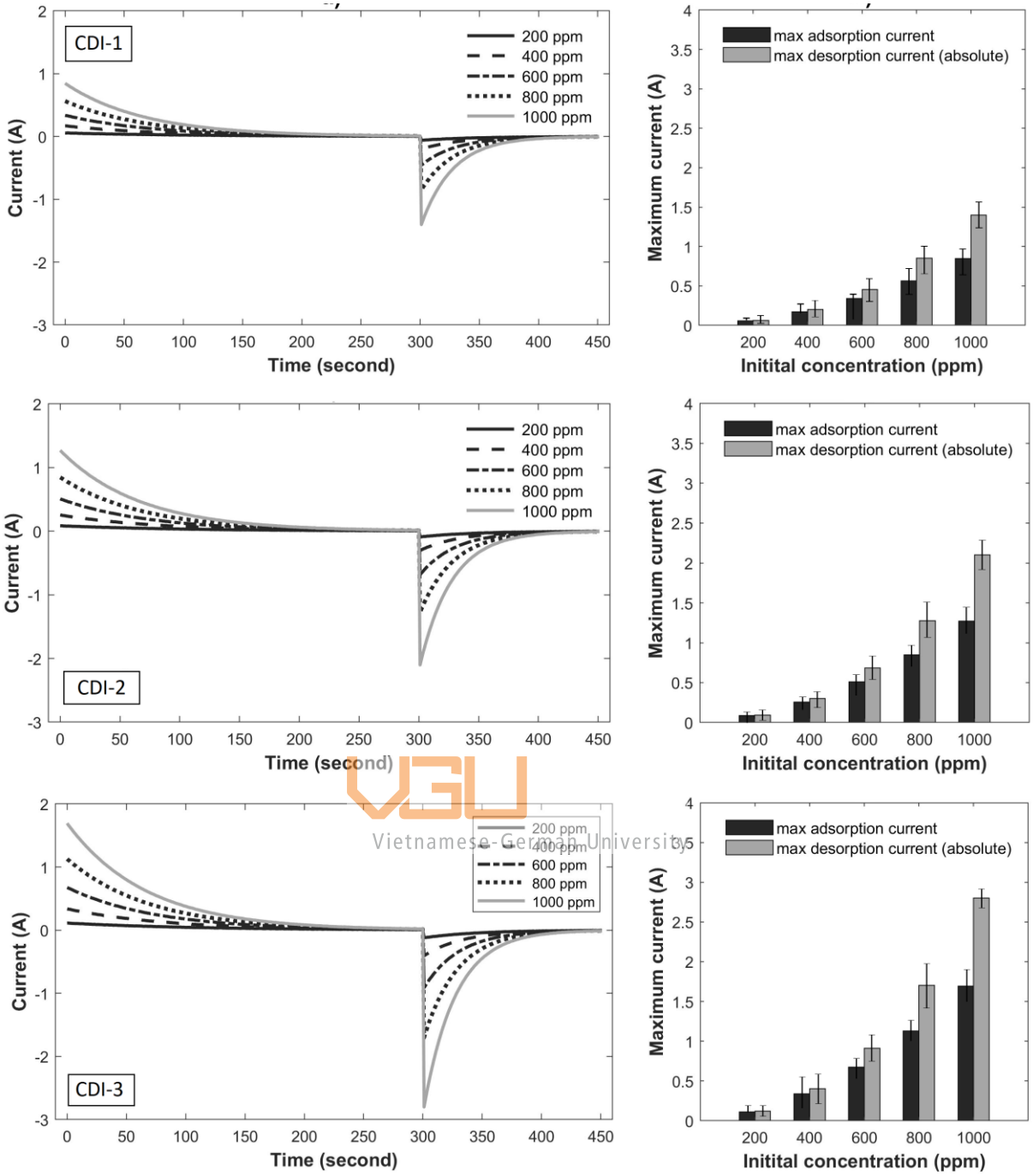

Figure 20. Electric behavior of different initial concentration operation.

Fig. 21c demonstrates the impact of initial water condition on suggesting that higher energy consumption per ion removed and lower energy recovery rate are observed at higher initial concentration. The energy requirements difference of 1.74 k J/g at 600 ppm and 1.47 kJ/g at 400 ppm can be explained by the low electrical resistance contributed by high saline water that contribute to larger current measurements in both adsorption and desorption phase which ultimately leads to higher energy usage. Additionally, when switching polarity of the power supply between the two operation phase, high desorption current will generate a larger

ohmic voltage drop. Henceforth, energy losses during desorption step are more prevalent in the case of infeed water with high salt soluble. Overall, the higher number of electrode pairs contributes to larger salt removal efficiency and generates better water quality with a downside of higher energy requirements in order to achieve that water quality.

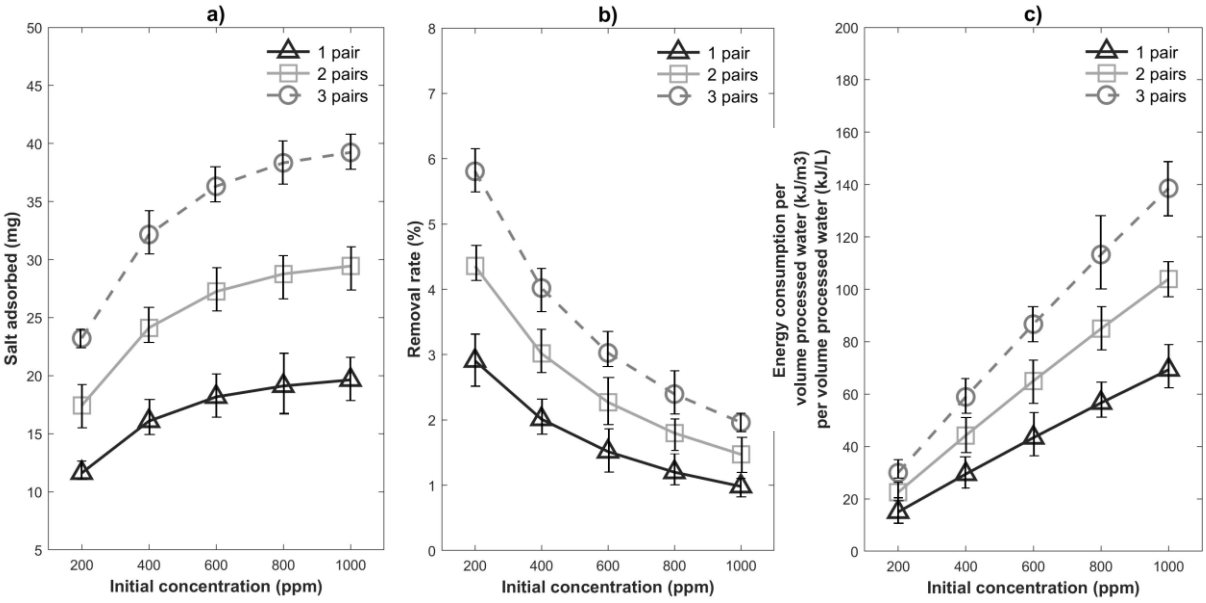

Figure 21. Comparison of different infeed TDS regarding: a) total mass adsorbed, b) removal rate and c) energy consumption.

4.1.2. Conclusion and result comparison

To better evaluate the CDI system, additional information from other research of similar electrode material [83] is included in table to compare result with the CDI-3 system. Only the CDI-3 is included in table 11 because of its highest performance amongst other systems. The reference CDI model include 50 pairs of activated carbon electrode of the same manufacturer, therefore are capable to process water with a much higher flow rate. Regardless, by using the adsorption capacity value, we can draw direct evaluation of the CDI-3 material.

Both models display similar trends of increasing adsorption capacity with higher initial TDS. The CDI-3, however, results in slightly lower capacity of the same concentration (200 ppm and 400 ppm). This can be explained by the higher voltage used in the reference study. Additionally, this reference study accompanied with the achieved results indicates a possibility to implement the CDI system in larger scale with limited drawbacks on the adsorption capacity.

Table 11. Comparison of initial concentration effect with other studies.

Case	Operation parameters					Performance values	
	V_{spacer} (mL)	*Capacitance* (F)	*Initial TDS* (ppm)	$V_{applied}$ (V)	*Flow rate* (mL/min)	*Adsorption capacity (mg/g)*	*Energy consumption* (kJ/m^3)
[83]	100	9930	200	1.3	4000	8.1	n.a.
			300			11.3	
			400			12.1	
CDI-3	6	397.2	200	1.2	400	7.3	29.9
			400			10.1	58.9
			600			11.3	86.7

4.2. Effects of applied voltage difference on desalination performance

4.2.1. Experiment data

To demonstrate the effect of applied voltage, CDI operation parameters is maintained at 600 ppm initial TDS and flow rate of 400mL/min while changing different voltage values from 1.0V – 1.4 V. Predictably, the adsorption behavior during operation of higher applied voltage outperform operation of lower voltage as the amount of ion adsorption is fundamentally reliant on amount of charge exchanged between electrodes (fig. 22). Similar to the previous experiment, by stacking multiple electrodes, the CDI system yields better desalination with the lowest effluent concentration of 559 ppm at 1.4V for CDI-3.

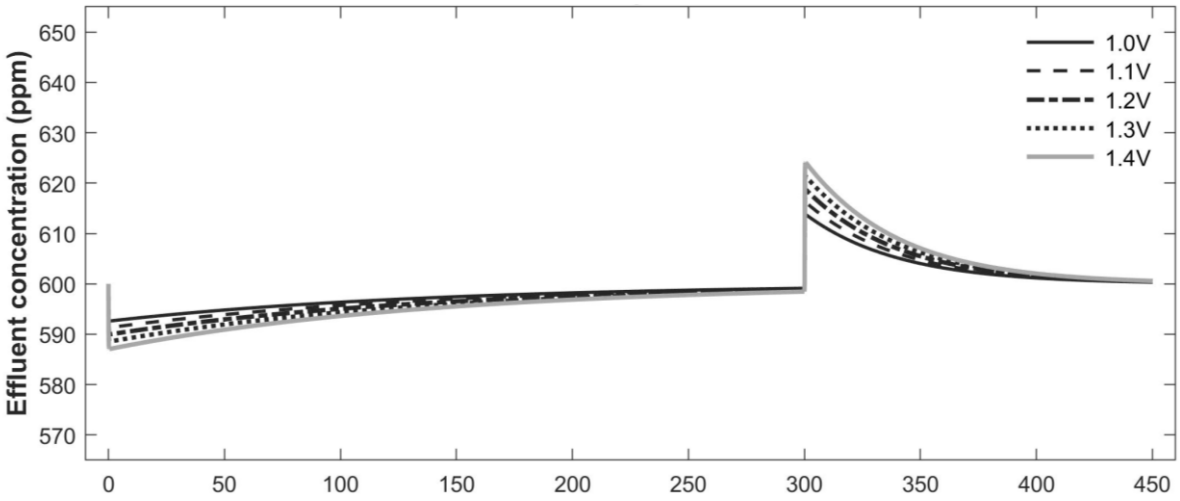

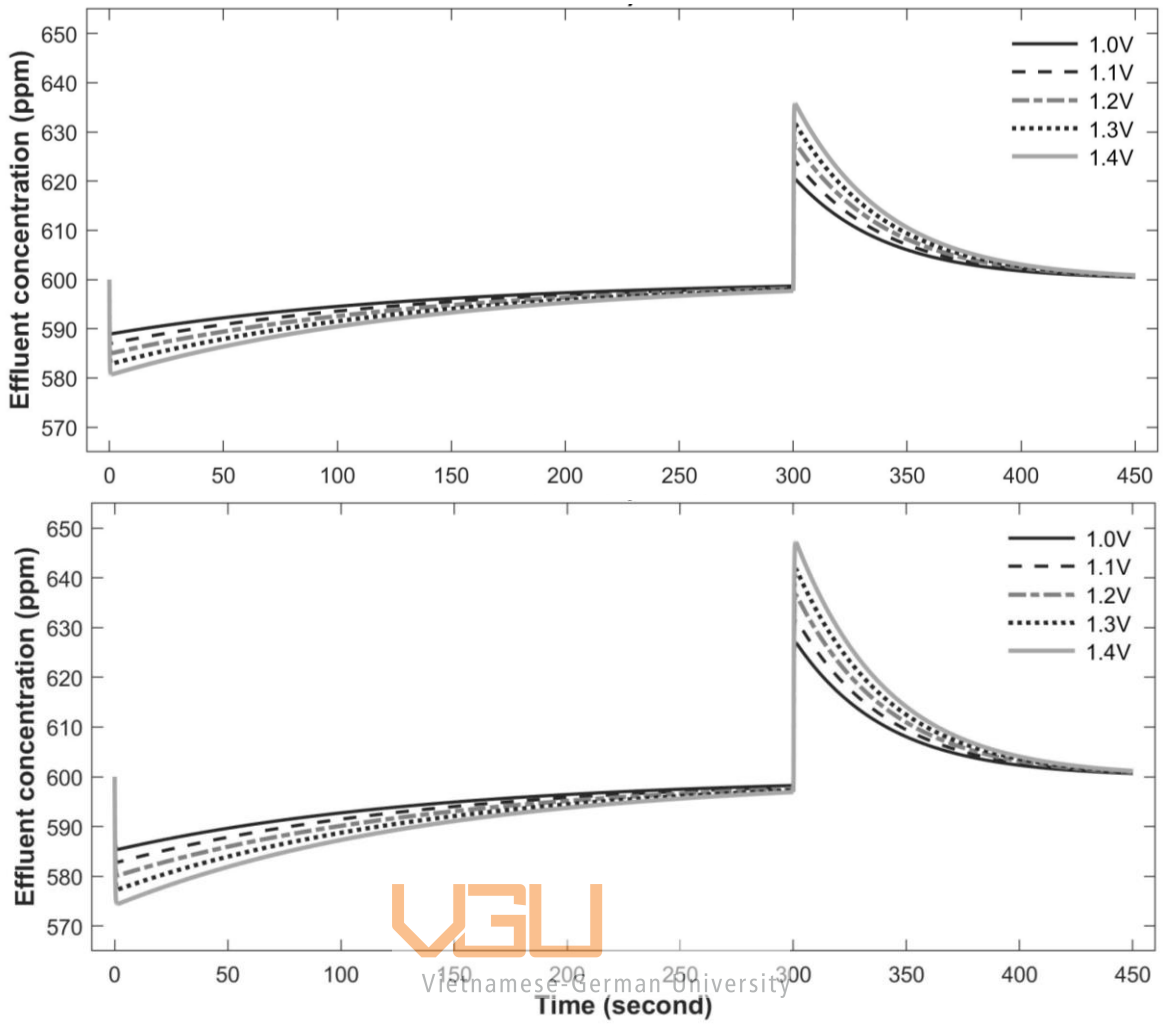

Figure 22. Effluent concentration at exit for different adsorption and desorption voltage (flow rate: 400mL/min; initial TDS: 600ppm; 66.7% WR).

Similar to how higher the initial TDS condition would increase the current density of the CDI electrode, increasing both adsorption and desorption voltage would also yield result of high ion exchange activity due to high current values (fig.23). The electrical current value, following the ohmic law, is linearly proportional to the applied voltage. As a consequence, the total amount of salt removed at 1.4V (~46.8 mg) for the triple pairs CDI is about 1.6 times higher than that at 1V (~4.8 mg) (fig. 24a).

However, different from the effect of varying infeed water concentration, the output water quality increase with increasing potential difference (fig. 24b). With the additional energy provided by higher voltage, a higher removal rate for a constant initial TDS can be achieved which is evidenced by the lower lowest concentration point. It is also important to note that with increasing potential different, when transitioning between the adsorption and

desorption phase, there will be larger ohmic loss due to rapid switching between the adsorption voltage and its negative value (fig. 24c).

Similar to how higher the initial TDS condition would increase the current density of the CDI electrode, increasing both adsorption and desorption voltage would also yield result of high ion exchange activity due to high current values (fig.23). The electrical current value, following the ohmic law, is linearly proportional to the applied voltage. As a consequent, the total amount of salt removed at 1.4V (~46.8 mg) for the triple pairs CDI is about 1.6 times higher than that at 1V (~4.8 mg) (fig. 24a).

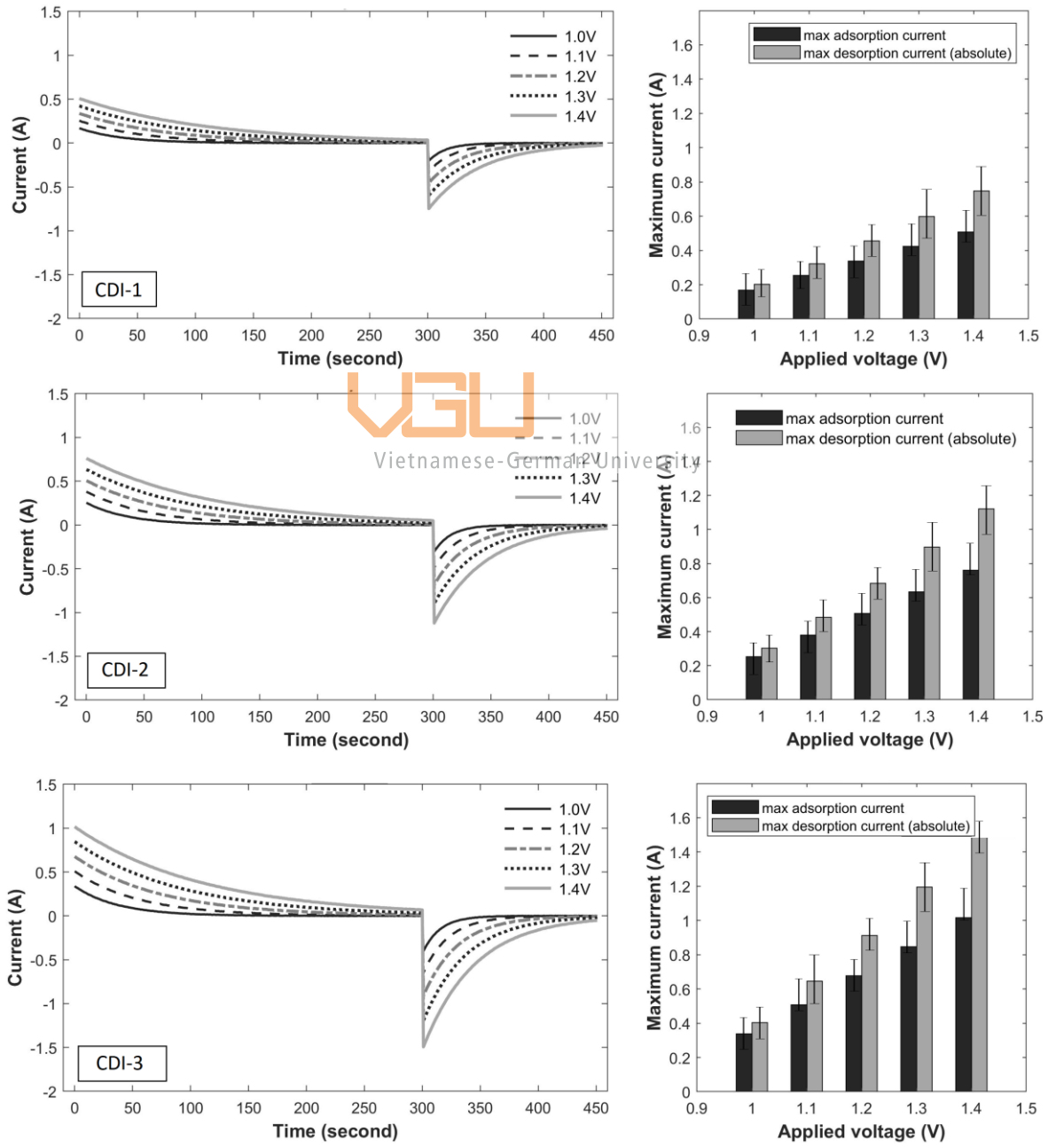

Figure 23. Electrical behavior of different applied voltage operation.

However, different from the effect of varying infeed water concentration, the output water quality increase with increasing potential difference (fig. 24b). With the additional energy provided by higher voltage, a higher removal rate for a constant initial TDS can be achieved which is evidenced by the lower lowest concentration point. It is also important to note that with increasing potential difference, when transitioning between the adsorption and desorption phase, there will be larger ohmic loss due to rapid switching between the adsorption voltage and its negative value (fig. 24c).

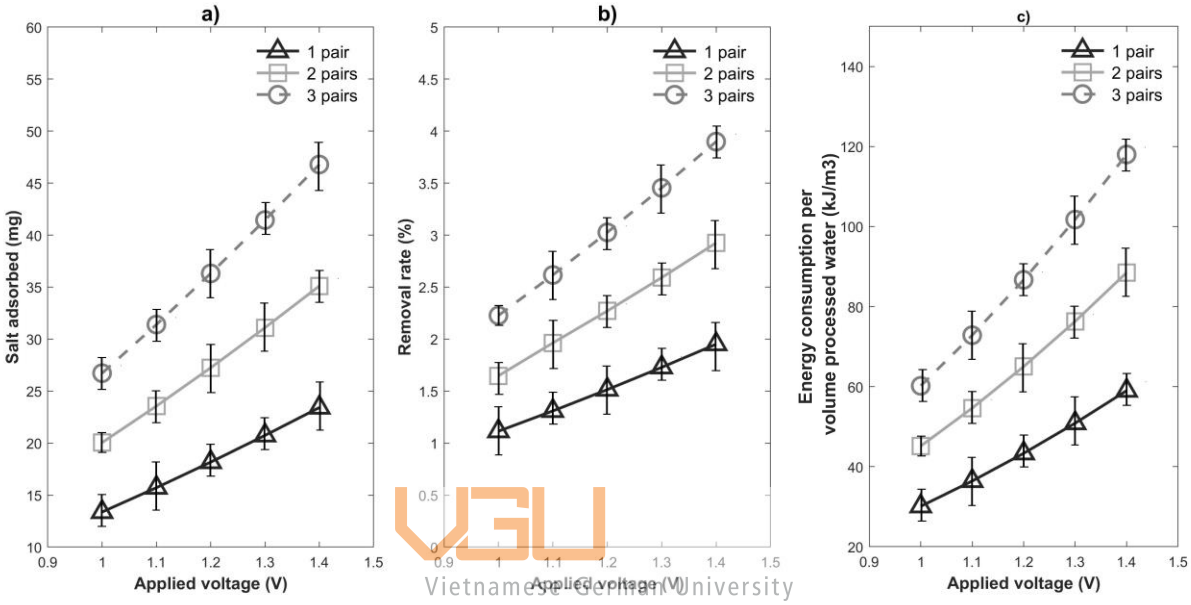

Figure 24. Comparison of different applied voltages regarding: a) total mass adsorbed, b) removal ratio and c) energy consumption.

4.2.2. Conclusion and result comparison

For this experiment we introduce a research case of a 6-cell CDI system with different charging conditions [84] to further evaluate performance of the CDI-3 model. In both system, higher adsorption capacity is observed with increasing applied voltage accompanied with higher energy consumption. The CDI-3 system operates under faster flow rate conditions result in slightly low desalination perform but, on the other hand, required much less energy to process the same amount of water. The lacking desalination rate can be explained due to the high input water velocity that provide less time for the ions solution to interact with the electrodes.

Table 12. Comparison of applied voltage effects with other studies.

Case	Operation parameters					Performance values	
	V_{spacer} (mL)	*Capacitance* (F)	*Initial TDS* (ppm)	$V_{applied}$ (V)	*Flow rate* (mL/min)	*Adsorption capacity (mg/g)*	*Energy consumption* (kJ/m^3)
[84]	12	n. a	292	0.4	40	5.8	18
				0.8		9.35	63
				1.2		16.36	153
CDI-3	6	397.2	600	1.0	400	8.4	60.2
				1.2		11.3	86.7
				1.4		14.6	118.0

4.3. Effects of changing flow rate on desalination performance

4.3.1. Experiment data

Flow rate is also an important control parameter that have substantial influence to the CDI desalination and energy performance. While maintaining operation conditions at 600ppm initial TDS and 1.2V of applied voltage, water stream with flow rate varies from 400 mL/min to 1200 mL/min enter the CDI. In fig. 25, records of the concentration measured at the output of the system showcase the tendency of larger salinity deviation at lower flow rate for all of the three CDI system. As lower flow rate would allow longer interaction between the solution and the electrode's surface and thus allowing more ion exchange activities.

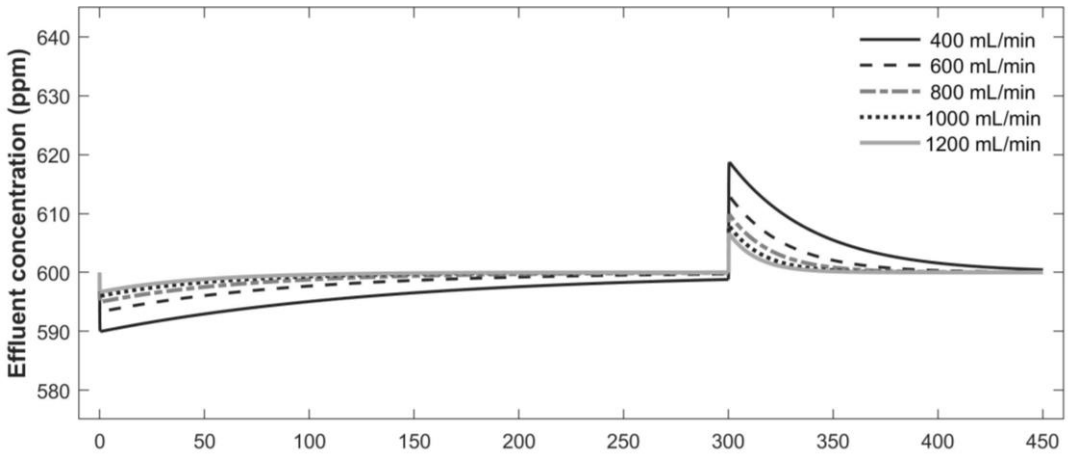

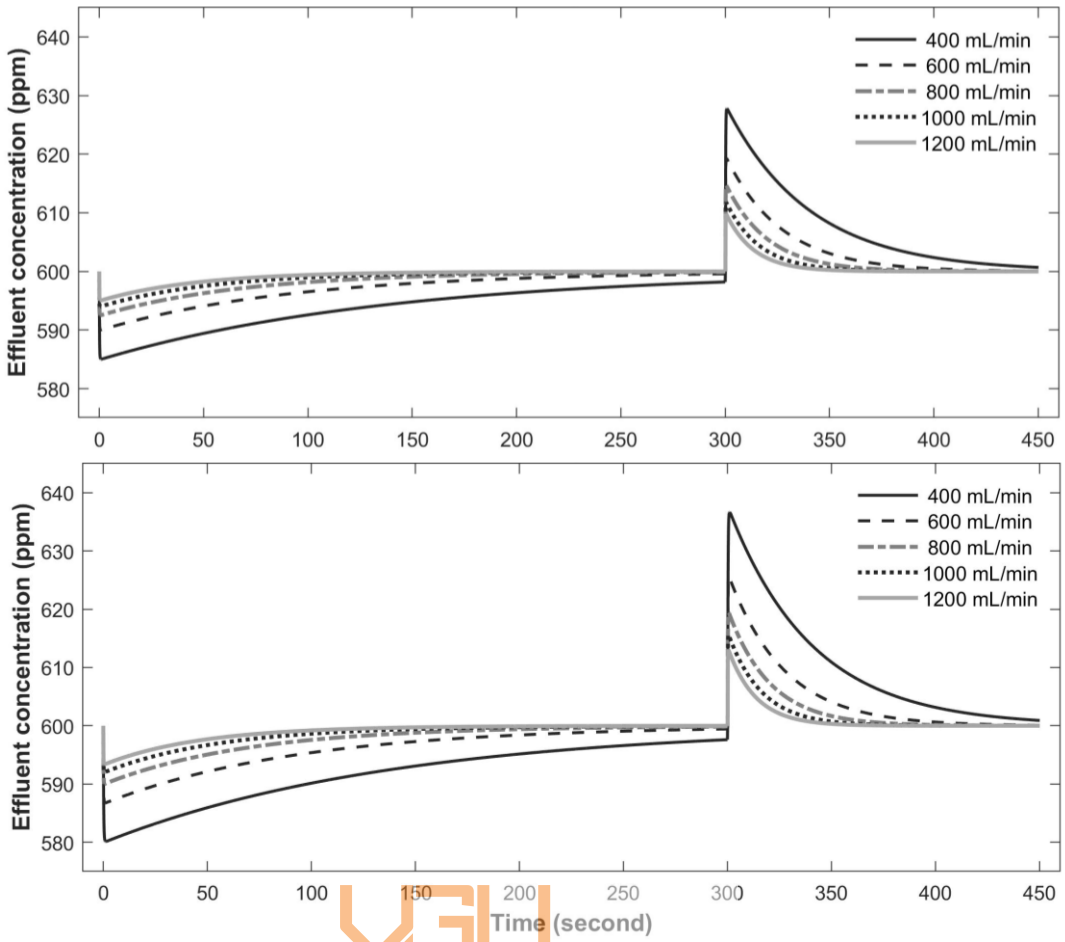

Figure 25. Effluent concentration at exit for different flow rate (Initial TDS: 600ppm; applied voltage: 1.2V; WR 66.7%).

Due to the fact that higher flow rate replenishes the CDI volume with water of initial TDS much quicker, the enhanced ion movements of the solution generate a lower internal resistance that inherently leads to higher currents (fig. 26). This is then further supported in fig. 27a when higher energy is needed to process a lower quantity of salt ions. For the triple pair CDI, the highest energy consumption of 15 kJ/g at 1200 mL/min is 3 times larger compared to the lowest energy consumption of 4.7 kJ/g at 400 mL/min. However, when is compared the energy consumption to the volume of treated water, because higher flow rate allows faster operation, the energy requirements decrease with increasing flow (fig. 27b).

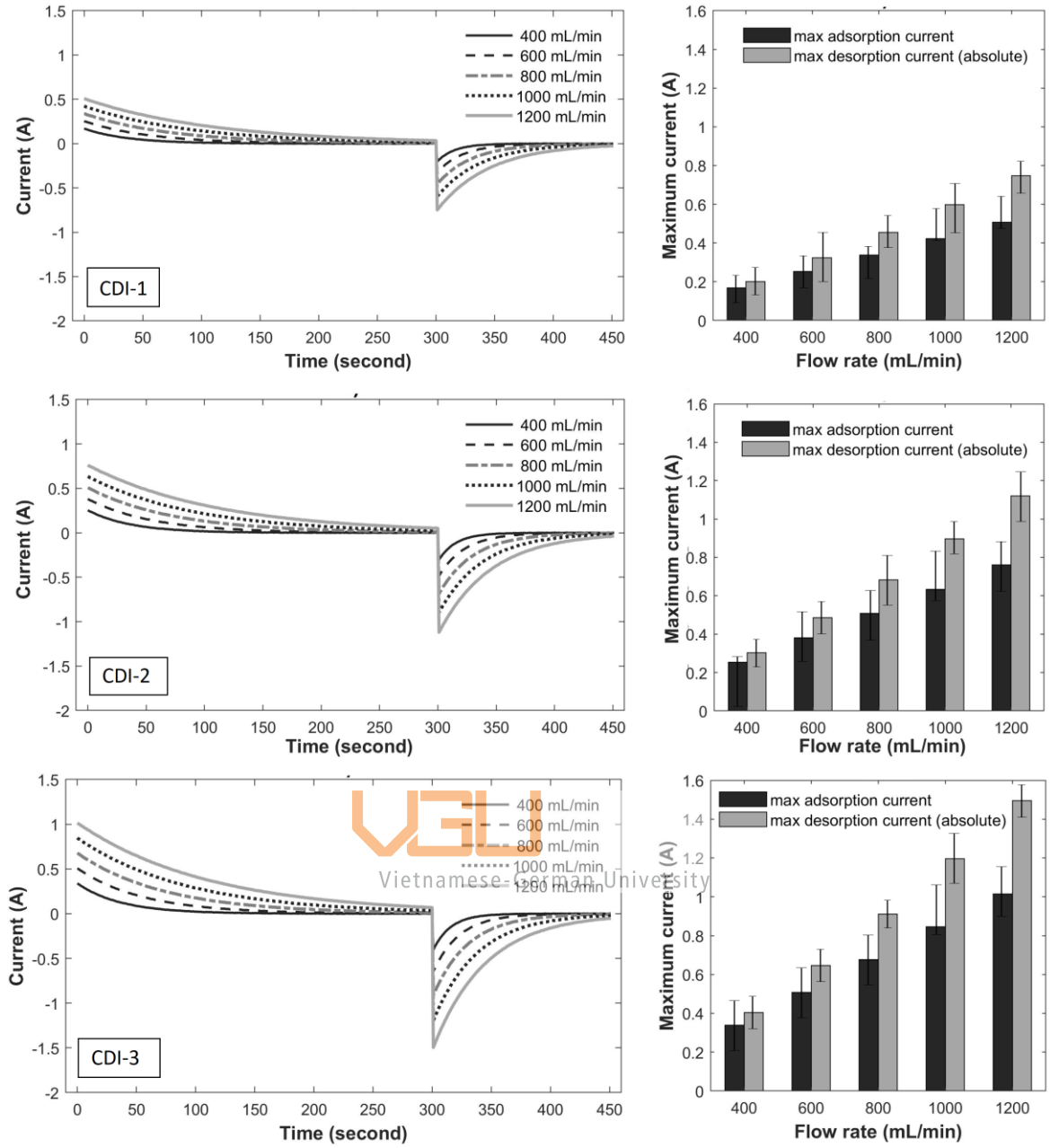

Figure 26. Electrical behavior of different flow rate operation.

Regarding removal performance, both the salt adsorption capacity and removal rate of the system can be improved by adjusting the flow rate value to a lower level (fig. 28a, b). While the amount of absorbed salt decrease almost linearly with increasing flow rate, the removal rate however shows great improvement at 400 mL/min. However, it is suggested that the flow rate should be in a reasonable range since too low flow rate would lead to slow operation and decrease the total water production. To achieved the desired water quality, different combination of other control parameter from the two previous sections can be used to best optimized the system.

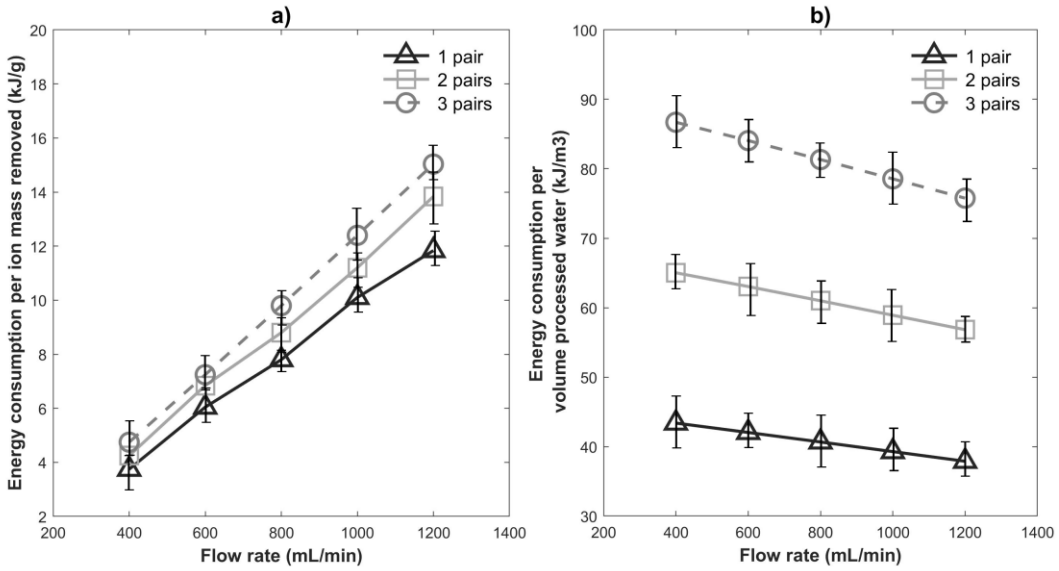

Figure 27. Comparison of different flow rate regarding: a) energy consumption per ion mass and b) energy consumption per volume.

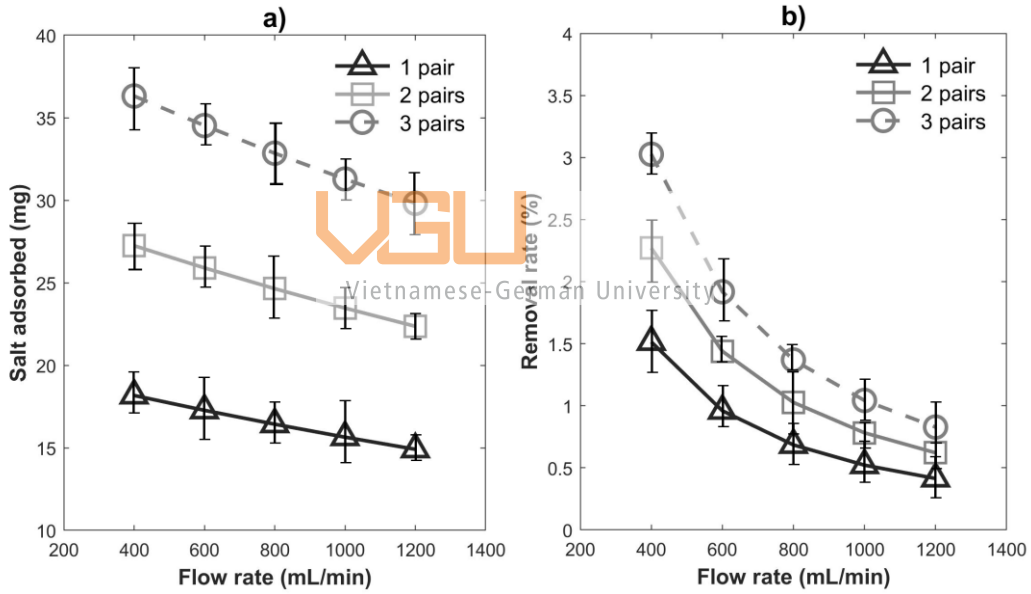

Figure 28. Comparison of different flow rate regarding: a) salt adsorbed and b) removal rate.

4.3.1. Conclusion and result comparison

We continue to compare our results with that from study [83]. Once again, the reference research outperforms our model due to its larger scale. Both studies depicted similar trends of better energy performance with increasing flow rate. Interestingly, in the pilot study, the flow rate parameter only have slight effects on removal rate of the system. However, if we look at fig. 28b, it is apparent that as the flow rate value continue to raise, the slope of the diagram decreases, suggesting that increasing feed water velocity to a certain point will no longer hold significant influence to the system.

Table 13. Comparison of flow rate effects with other studies.

Case	Operation parameters					Performance values	
	V_{spacer} (mL)	*Capacitance* (F)	*Initial TDS* (ppm)	$V_{applied}$ (V)	*Flow rate* (mL/min)	*Removal rate* *(%)*	*Energy consumption* (kJ/m^3)
[83]	100	9930	150	1.3	2000	94	756
					3000	97	612
					4000	94	540
CDI-3	6	397.2	600	1.2V	400	3.1	86.7
					800	1.4	81.3
					1200	0.8	75.7

4.4. Effects of different discharging mode on desalination performance

4.4.1. Experiment data

The discharging phase of CDI operation is often overlooked when designing system due to the fact that it does not contribute any advancement to the system removal efficiency. In fact, the discharge phase is attributed to the stability of the operating system, including electrode regeneration and energy recovery. We consider for this experiment two different discharging modes, i.e., reverse voltage discharge (RVD) and zero voltage discharge. The RVD mode involves switching the polarities of the electrode to create a negative potential difference, as to the positive potential difference during charging phase. The ZVD mode, on the other hand, a zero potential difference is applied by creating a short-circuit across the terminals. Fig. 29 records the concentration measurement of the desorption phase with different discharge mode and time for comparison.

Through observation, by substituting partial of the original RVD discharging period with different combination of ZVD and RVD method, we can achieve better regeneration. Results from fig. 30a indicate the fastest regeneration of CDI electrode is found with 50s of ZVD followed by a 100s of RVD. Other configuration of combined ZVD and RVD, on the other hand are proven to be and results in incomplete regeneration with only 50% regeneration rate. As for the energy consumption, reverse voltage discharge proves to be more ineffective as it has the highest requirement of 86.9 kJ/m^3 (CDI-3). Besides the obvious energy reduction due to decrease of voltage supply duration, by adding a transition process of short-circuiting the system before apply the reverse voltage, we can prevent more ohmic loss caused by the rapid switching of potential values (fig. 30b).

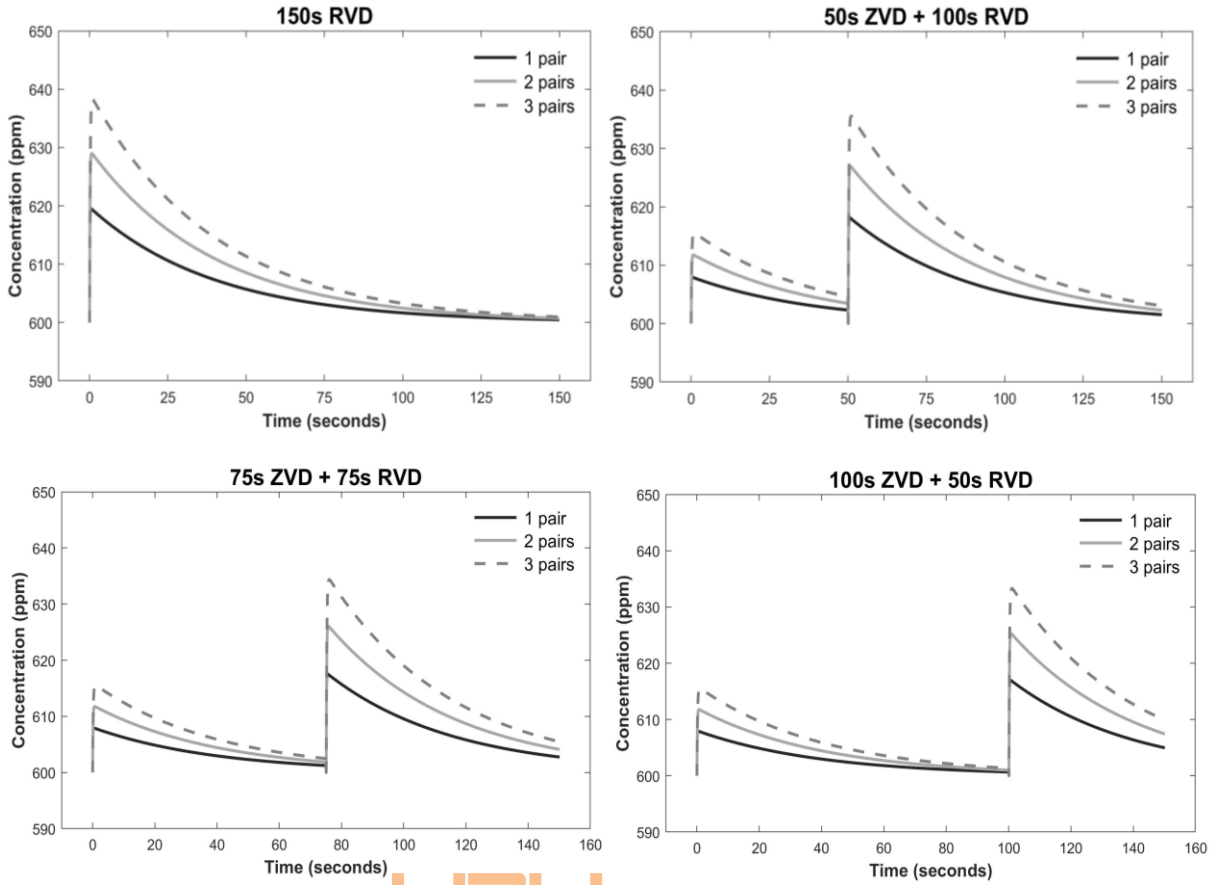

Figure 29. Effluent concentration at exit during desorption phase for discharge mode.

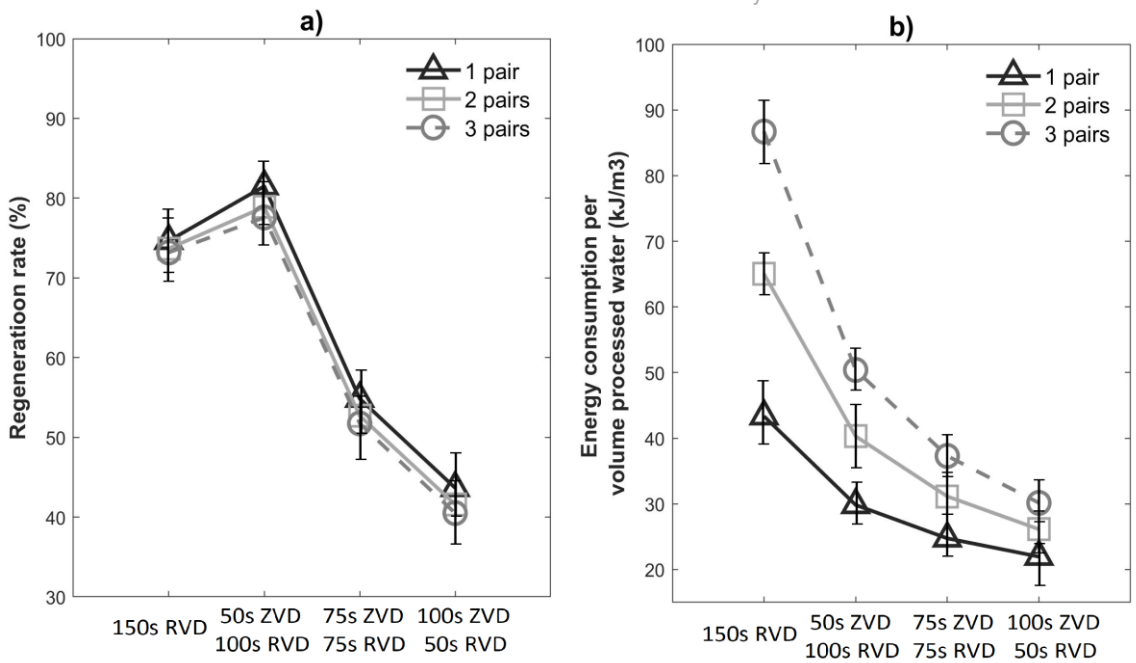

Figure 30. Comparison of different discharge mode regarding: a) electrode regeneration rate and b) energy consumption.

4.4.2. Conclusion and result comparison

The premise for comparative evaluation of this experiment is base from one study by Q. Yao of an activated carbon CDI cells. This paper provides result of regeneration rate for either full RVD or ZVD process during a 900 seconds discharge period. At first glance, the CDI-3 cell underperform with only 77.6% regeneration is achieved (table 14). However, when taking consideration of the operating flow rate is much higher and shorter discharge duration than the values from [85], the CDI-3 is proven to be more effective timewise with faster desorption duration. For higher regeneration rate to be achieve, modification such as increasing discharging time or reducing feed velocity can be done to get the desired result.

Table 14. Comparison of discharging mode effects with other study.

Case	**Operation parameters**					**Performance values**	
	Discharge method	$V_{applied}$ (V)	**RVD time**	**ZVD time**	***Flow rate*** (mL/min)	***Regeneration rate (%)***	***Energy consumption*** (kJ/m^3)
[85]	RVD	1.2	900	0	30	82	n. a
	ZVD	0	0	900	45	65	n. a
CDI-3	RVD	1.2	150	0	400	73.2	86.7
	RVD+ZVD	1.2	100	50		77.6	81.3
	RVD+ZVD	1.2	50	100		40.5	75.7

5. Conclusion

Investigation provided in this paper showcases the possible configurations when design a CDI system. Desirable results can be achieved by tuning. Although, lower concentration feedwater has higher removal, it is not recommended for adsorption cycle due to the fact that majority of CDI operation is performed with brackish water (~1000 ppm). Instead, applying low TDS feedwater during the desorption would be more realistically appropriate as it would provide faster regeneration. High adsorption capacity of 11.3 mg/g is observed at 400mL/min flowrate and 1.2V applied voltage, which is higher than the conventional activated carbon. Additionally, while short-circuiting the system before reversing the voltage potential of the CDI provide better regeneration with less energy requirement, extending the short-circuit period would results in incomplete regeneration and should be avoided as a whole.

The CDI performance shows great potential and many optimization approaches for further advancement. The process is applicable for automation where each operational metric can be controlled by simple programing. This allows stable operation to product consistent water quality output.

.

6. References

[1] H. D. M. Vo, M. T. T. Tran, and L. T. Nguyen, "Tai nguyen nuoc va hien trang su dung nuoc," Ho Chi Minh Nong Lam University, Ho Chi Minh, 2013.

[2] T. N. M. T. Bo, "Bao cao moi truong quoc gia 2010: tong quan moi truong Viet Nam," (in Vietnamese), 2010.

[3] H. V. Hoang and M. T. X. Tran. "Tac dong cua qua trinh nuoc bien dang doi voi vung cua song, ven bien dong bang Nam Bo va dinh huong nhung hanh dong ung pho." Institute of Water and Environment. http://iwe.vn/p1c3/p2c8/n32/-tac-dong-cua-qua-trinh-nuoc-bien-dang-doi-voi-vung-cua-song-ven-bien-dong-bang/ (accessed.

[4] L. V. Tuan, V. V. Thang, and T. D. Trong, "Danh gia hiem hoa, tinh de bi ton thuong va rui ro do xam nhap man tren khu vuc dong bang son Cuu Long," IMHEN, 2021.

[5] G. Micale, L. Rizzuti, and A. Cipollina, "Seawater Desalination for Freshwater Production," in *Seawater desalination: Conventional and Renewable Energy Processes*, vol. 1. Berlin: Springer, 2009, ch. 1, pp. 1-15.

[6] WHO, "Guidelines for drinking-water quality," *WHO chronicle,* vol. 38, no. 4, 2011.

[7] N. D. o. Health, "Salt and Drinking Water," 2019.

[8] C. Wangnick, "1998 IDA Worldwide Desalting Plant Inventory Report. No. 15," *Wangnick Consulting GMBH,* 1988.

[9] A. D. Khawaji, I. K. Kutubkhanah, and J.-M. Wie, "Advances in seawater desalination technologies," *Desalination,* vol. 221, no. 3, 2008.

[10] S. A. Kalogirou, "Solar Desalination System," in *Solar Energy Engineering* 2ed. Boston: Academic Press, 2014, ch. 8, pp. 431-479.

[11] K. R. Khalilpour, "Energy-Water Nexus: Renewable-Integrated Hybridized Desalination Systems," in *Polygeneration with polystorage: for chemical and energy hubs*: Academic Press, 2018, ch. 13, pp. 409-458.

[12] P. Sharan, T. J. Yoon, S. M. Jaffe, T. Ju, R. P. Currier, and A. T. Findikoglu, "Can capacitive deionization outperform reverse osmosis for brackish water desalination?," *Cleaner Engineering and Technology,* vol. 3, p. 100102, 2021.

[13] M. J. Brandt, K. M. Johnson, A. J. Elphinston, and D. D. Ratnayaka, "Specialized and Advanced Water Treatment Processes," in *Twort's water supply*, 7 ed.: Butterworth-Heinemann, 2016, ch. 10, pp. 407-473.

[14] S. Moran, "Clean water unit operation design: Physical processes," in *An Applied Guide to Water and Effluent Treatment Plant Design*: Butterworth-Heinemann, 2018, ch. 7, pp. 69-100.

[15] N. Ghaffour, T. M. Missimer, and G. L. Amy, "Technical review and evaluation of the economics of water desalination: current and future challenges for better water supply sustainability," *Desalination,* vol. 309, pp. 197-207, 2013.

[16] J. W. Blair and G. W. Murphy, "Electrochemical demineralization of water with porous electrodes of large surface area," ACS Publications, 1960.

[17] P. Biesheuvel *et al.*, "Capacitive Deionization--defining a class of desalination technologies," *arXiv preprint arXiv:1709.05925,* 2017.

[18] N. Lee, M.-L. Liu, M.-C. Wu, T.-H. Chen, and C.-H. Hou, "The effect of redox potential on the removal characteristic of divalent cations during activated carbon-based capacitive deionization," *Chemosphere,* vol. 274, p. 129762, 2021.

[19] C. Zhang, X. Wang, H. Wang, X. Wu, and J. Shen, "A positive-negative alternate adsorption effect for capacitive deionization in nano-porous carbon aerogel electrodes to enhance desalination capacity," *Desalination,* vol. 458, pp. 45-53, 2019.

[20] Y. Wimalasiri and L. Zou, "Carbon nanotube/graphene composite for enhanced capacitive deionization performance," *Carbon,* vol. 59, pp. 464-471, 2013.

[21] T. N. Tuan, "Enhancing water softening performance in capacitive deionization by using activated waste coffee ground electrode," *Industry and Trade Magazine,* vol. 16, pp. 279-286, 2019. [Online]. Available: https://tapchicongthuong.vn/bai-viet/enhancing-water-softening-performance-in-capacitive-deionization-by-using-activated-waste-coffee-groumd-electrode-72968.htm.

[22] T. N. Pham *et al.*, "Coconut shell-derived activated carbon and carbon nanotubes composite: a promising candidate for capacitive deionization electrode," *Synthetic Metals,* vol. 265, p. 116415, 2020.

[23] J.-B. Lee, K.-K. Park, H.-M. Eum, and C.-W. Lee, "Desalination of a thermal power plant wastewater by membrane capacitive deionization," *Desalination,* vol. 196, no. 1-3, pp. 125-134, 2006.

[24] J. Kang, T. Kim, K. Jo, and J. Yoon, "Comparison of salt adsorption capacity and energy consumption between constant current and constant voltage operation in capacitive deionization," *Desalination,* vol. 352, pp. 52-57, 2014.

[25] Y. Qu *et al.*, "Energy consumption analysis of constant voltage and constant current operations in capacitive deionization," *Desalination,* vol. 400, pp. 18-24, 2016.

[26] E. M. Remillard, A. N. Shocron, J. Rahill, M. E. Suss, and C. D. Vecitis, "A direct comparison of flow-by and flow-through capacitive deionization," *Desalination,* vol. 444, pp. 169-177, 2018.

[27] K. M. Barcelos, K. S. Oliveira, D. S. Silva, E. A. Urquieta-González, and L. A. Ruotolo, "Efficient and stable operation of capacitive deionization assessed by electrode and membrane asymmetry," *Electrochimica Acta,* vol. 388, p. 138631, 2021.

[28] Y. Liu *et al.*, "One-step turning leather wastes into heteroatom doped carbon aerogel for performance enhanced capacitive deionization," *Microporous and Mesoporous Materials,* vol. 303, p. 110303, 2020.

[29] C. Kim, P. Srimuk, J. Lee, S. Fleischmann, M. Aslan, and V. Presser, "Influence of pore structure and cell voltage of activated carbon cloth as a versatile electrode material for capacitive deionization," *Carbon,* vol. 122, pp. 329-335, 2017.

[30] G. Wang *et al.*, "Activated carbon nanofiber webs made by electrospinning for capacitive deionization," *Electrochimica Acta,* vol. 69, pp. 65-70, 2012.

[31] X. Wei, X. Li, C. Lv, X. Mo, and K. Li, "Hierarchically yolk-shell porous carbon sphere as an electrode material for high-performance capacitive deionization," *Electrochimica Acta,* vol. 354, p. 136590, 2020.

[32] S. Zhang, Y. Wang, X. Han, Y. Cai, and S. Xu, "Optimizing the fabrication of carbon nanotube electrode for effective capacitive deionization via electrophoretic deposition strategy," *Progress in Natural Science: Materials International,* vol. 28, no. 2, pp. 251-257, 2018.

[33] B. Xu *et al.*, "Electro-enhanced adsorption of ammonium ions by effective graphene-based electrode in capacitive deionization," *Separation and Purification Technology,* vol. 250, p. 117243, 2020.

[34] S. D. Datar, K. Mohanapriya, D. J. Ahirrao, and N. Jha, "Comparative study of electrosorption performance of solar reduced graphene oxide in flow-between and flow-through capacitive deionization architectures," *Separation and Purification Technology,* vol. 257, p. 117972, 2021.

[35] C. Huyskens, J. Helsen, W. J. Groot, and A. B. de Haan, "Cost evaluation of large-scale membrane capacitive deionization for biomass hydrolysate desalination," *Separation and Purification Technology,* vol. 146, pp. 294-300, 2015.

[36] C.-H. Hou, N.-L. Liu, H.-L. Hsu, and W. Den, "Development of multi-walled carbon nanotube/poly (vinyl alcohol) composite as electrode for capacitive deionization," *Separation and Purification Technology,* vol. 130, pp. 7-14, 2014.

[37] X. Zhang and D. Reible, "Theoretical Analysis of Constant Voltage Mode Membrane Capacitive Deionization for Water Softening," *Membranes,* vol. 11, no. 4, p. 231, 2021.

[38] S.-M. Jung, J.-H. Choi, and J.-H. Kim, "Application of capacitive deionization (CDI) technology to insulin purification process," *Separation and purification technology,* vol. 98, pp. 31-35, 2012.

[39] K. Lellala, "Sulphur Embedded On In-Situ Carbon Nanodisc Decorated On Graphene Sheets For Efficient Photocatalytic Activity And Capacitive Deionization Method For Heavy Metal Removal," *Journal of Materials Research and Technology,* 2021.

[40] M. A. Ahmed and S. Tewari, "Capacitive deionization: Processes, materials and state of the technology," *Journal of Electroanalytical Chemistry,* vol. 813, pp. 178-192, 2018.

[41] S. Porada, R. Zhao, A. Van Der Wal, V. Presser, and P. Biesheuvel, "Review on the science and technology of water desalination by capacitive deionization," *Progress in materials science,* vol. 58, no. 8, pp. 1388-1442, 2013.

[42] Q.-D. Chen, S.-H. Shyu, and W.-L. Li, "An overlapped electrical double layer model for aqueous electrolyte lubrication with asymmetric surface electric potentials," *Tribology International,* vol. 147, p. 106283, 2020.

[43] Y. Oren, "Capacitive deionization (CDI) for desalination and water treatment—past, present and future (a review)," *Desalination,* vol. 228, no. 1-3, pp. 10-29, 2008.

[44] M. H. Nguyen. "Periodic Trends in Ionic Radii." LibreTexts. https://chem.libretexts.org/Bookshelves/Inorganic_Chemistry/Supplemental_Modules_and_Websites_(Inorganic_Chemistry)/Descriptive_Chemistry/Periodic_Trends_of_Elemental_Properties/Periodic_Trends_in_Ionic_Radii (accessed.

[45] Z.-y. Li, J.-y. Li, R.-k. Xu, Z.-n. Hong, and Z.-d. Liu, "Streaming potential method for characterizing the overlapping of diffuse layers of the electrical double layers between oppositely charged particles," *Colloids and Surfaces A: Physicochemical and Engineering Aspects,* vol. 478, pp. 22-29, 2015.

[46] S. Maass, F. Finsterwalder, G. Frank, R. Hartmann, and C. Merten, "Carbon support oxidation in PEM fuel cell cathodes," *Journal of Power Sources,* vol. 176, no. 2, pp. 444-451, 2008.

[47] H.-S. Oh *et al.*, "On-line mass spectrometry study of carbon corrosion in polymer electrolyte membrane fuel cells," *Electrochemistry Communications,* vol. 10, no. 7, pp. 1048-1051, 2008.

[48] I. Cohen, E. Avraham, Y. Bouhadana, A. Soffer, and D. Aurbach, "Long term stability of capacitive de-ionization processes for water desalination: The challenge of positive electrodes corrosion," *Electrochimica Acta,* vol. 106, pp. 91-100, 2013.

[49] F. Duan, X. Du, Y. Li, H. Cao, and Y. Zhang, "Desalination stability of capacitive deionization using ordered mesoporous carbon: Effect of oxygen-containing surface groups and pore properties," *Desalination,* vol. 376, pp. 17-24, 2015.

[50] D. Lu, W. Cai, and Y. Wang, "Optimization of the voltage window for long-term capacitive deionization stability," *Desalination,* vol. 424, pp. 53-61, 2017.

[51] J. Yu, K. Jo, T. Kim, J. Lee, and J. Yoon, "Temporal and spatial distribution of pH in flow-mode capacitive deionization and membrane capacitive deionization," *Desalination,* vol. 439, pp. 188-195, 2018.

[52] S. Porada, A. Shrivastava, P. Bukowska, P. Biesheuvel, and K. C. Smith, "Nickel hexacyanoferrate electrodes for continuous cation intercalation desalination of brackish water," *Electrochimica Acta,* vol. 255, pp. 369-378, 2017.

[53] C. Zhang, D. He, J. Ma, W. Tang, and T. D. Waite, "Faradaic reactions in capacitive deionization (CDI)-problems and possibilities: A review," *Water research,* vol. 128, pp. 314-330, 2018.

[54] W. Tang, D. He, C. Zhang, P. Kovalsky, and T. D. Waite, "Comparison of Faradaic reactions in capacitive deionization (CDI) and membrane capacitive deionization (MCDI) water treatment processes," *Water research,* vol. 120, pp. 229-237, 2017.

[55] C. Zhang, D. He, J. Ma, W. Tang, and T. D. Waite, "Comparison of faradaic reactions in flow-through and flow-by capacitive deionization (CDI) systems," *Electrochimica Acta,* vol. 299, pp. 727-735, 2019.

[56] N. Holubowitch, A. Omosebi, X. Gao, J. Landon, and K. Liu, "Quasi-steady-state polarization reveals the interplay of capacitive and Faradaic processes in capacitive deionization," *ChemElectroChem,* vol. 4, no. 9, pp. 2404-2413, 2017.

[57] Y. Uematsu, R. R. Netz, and D. J. Bonthuis, "The effects of ion adsorption on the potential of zero charge and the differential capacitance of charged aqueous interfaces," *Journal of Physics: Condensed Matter,* vol. 30, no. 6, p. 064002, 2018.

[58] K.-L. Yang, S. Yiacoumi, and C. Tsouris, "Electrosorption capacitance of nanostructured carbon aerogel obtained by cyclic voltammetry," *Journal of Electroanalytical Chemistry,* vol. 540, pp. 159-167, 2003.

[59] J. Poon, C. Batchelor-McAuley, K. Tschulik, and R. G. Compton, "Single graphene nanoplatelets: capacitance, potential of zero charge and diffusion coefficient," *Chemical science,* vol. 6, no. 5, pp. 2869-2876, 2015.

[60] E. Toledo-Carrillo, X. Zhang, K. Laxman, and J. Dutta, "Asymmetric electrode capacitive deionization for energy efficient desalination," *Electrochimica Acta,* vol. 358, p. 136939, 2020.

[61] T. Wu *et al.*, "Surface-treated carbon electrodes with modified potential of zero charge for capacitive deionization," *Water research,* vol. 93, pp. 30-37, 2016.

[62] X. Gao *et al.*, "Capacitive deionization using symmetric carbon electrode pairs," *Environmental Science: Water Research & Technology,* vol. 5, no. 4, pp. 660-671, 2019.

[63] J. Choi, J. Kim, and S. Hong, "Staged voltage mode in membrane capacitive deionization: Comparison with constant voltage and constant current modes," *Desalination,* vol. 479, p. 114327, 2020.

[64] P. Shui and E. Alhseinat, "Quantitative insight into the effect of ions size and electrodes pores on capacitive deionization performance," *Electrochimica Acta,* vol. 329, p. 135176, 2020.

[65] L. Zou, L. Li, H. Song, and G. Morris, "Using mesoporous carbon electrodes for brackish water desalination," *Water research,* vol. 42, no. 8-9, pp. 2340-2348, 2008.

[66] C. Macías, P. Lavela, G. Rasines, M. Zafra, J. Tirado, and C. Ania, "Improved electro-assisted removal of phosphates and nitrates using mesoporous carbon aerogels with controlled porosity," *Journal of Applied Electrochemistry,* vol. 44, no. 8, pp. 963-976, 2014.

[67] L. Han, K. Karthikeyan, M. A. Anderson, and K. B. Gregory, "Exploring the impact of pore size distribution on the performance of carbon electrodes for capacitive deionization," *Journal of colloid and interface science,* vol. 430, pp. 93-99, 2014.

[68] A. Volkov, S. Paula, and D. Deamer, "Two mechanisms of permeation of small neutral molecules and hydrated ions across phospholipid bilayers," *Bioelectrochemistry and bioenergetics,* vol. 42, no. 2, pp. 153-160, 1997.

[69] G. Amy *et al.*, *Treatability of perchlorate-containing water by RO, NF and UF membranes*. IWA Publishing, 2004.

[70] H. Ohtaki and T. Radnai, "Structure and dynamics of hydrated ions," *Chemical reviews,* vol. 93, no. 3, pp. 1157-1204, 1993.

[71] M. Y. Kiriukhin and K. D. Collins, "Dynamic hydration numbers for biologically important ions," *Biophysical chemistry,* vol. 99, no. 2, pp. 155-168, 2002.

[72] W. Huang, Y. Zhang, S. Bao, R. Cruz, and S. Song, "Desalination by capacitive deionization process using nitric acid-modified activated carbon as the electrodes," *Desalination,* vol. 340, pp. 67-72, 2014.

[73] O. Sufiani, H. Tanaka, K. Teshima, R. L. Machunda, and Y. A. Jande, "Enhanced electrosorption capacity of activated carbon electrodes for deionized water production through capacitive deionization," *Separation and Purification Technology,* vol. 247, p. 116998, 2020.

[74] R. Niu, H. Li, Y. Ma, L. He, and J. Li, "An insight into the improved capacitive deionization performance of activated carbon treated by sulfuric acid," *Electrochimica Acta,* vol. 176, pp. 755-762, 2015.

[75] C. Lu and H. Chiu, "Chemical modification of multiwalled carbon nanotubes for sorption of Zn2+ from aqueous solution," *Chemical Engineering Journal,* vol. 139, no. 3, pp. 462-468, 2008.

[76] X. Song, H. Liu, L. Cheng, and Y. Qu, "Surface modification of coconut-based activated carbon by liquid-phase oxidation and its effects on lead ion adsorption," *Desalination,* vol. 255, no. 1-3, pp. 78-83, 2010.

[77] T. A. Langston and R. D. Granata, "Influence of nitric acid treatment time on the mechanical and surface properties of high-strength carbon fibers," *Journal of Composite Materials,* vol. 48, no. 3, pp. 259-276, 2014.

[78] X. Liu and J. Wang, "Electro-assisted adsorption of Cs (I) and Co (II) from aqueous solution by capacitive deionization with activated carbon cloth/graphene oxide composite electrode," *Science of The Total Environment,* vol. 749, p. 141524, 2020.

[79] Y. Liu *et al.*, "MnO2 decorated porous carbon derived from Enteromorpha prolifera as flow-through electrode for dual-mode capacitive deionization," *Desalination,* vol. 504, p. 114977, 2021.

[80] B. Krüner *et al.*, "Hydrogen-treated, sub-micrometer carbon beads for fast capacitive deionization with high performance stability," *Carbon,* vol. 117, pp. 46-54, 2017.

[81] F. Yang *et al.*, "Flow-electrode capacitive deionization: a review and new perspectives," *Water Research,* p. 117222, 2021.

[82] S. A. Hawks *et al.*, "Performance metrics for the objective assessment of capacitive deionization systems," *Water research,* vol. 152, pp. 126-137, 2019.

[83] P. Dorji, D. I. Kim, S. Hong, S. Phuntsho, and H. K. Shon, "Pilot-scale membrane capacitive deionisation for effective bromide removal and high water recovery in seawater desalination," *Desalination,* vol. 479, p. 114309, 2020.

[84] L. Chen, X. Yin, L. Zhu, and Y. Qiu, "Energy recovery and electrode regeneration under different charge/discharge conditions in membrane capacitive deionization," *Desalination,* vol. 439, pp. 93-101, 2018.

[85] Q. Yao and H. L. Tang, "Effect of desorption methods on electrode regeneration performance of capacitive deionization," *Journal of Environmental Engineering,* vol. 143, no. 9, p. 04017047, 2017.